STRUCTURAL STUDIES OF SELF-ASSEMBLED Cu(II), Ni(II) AND Cd(II) COORDINATION POLYMERS FABRICATED WITH AMINE LIGANDS AND DICARBOXYLIC ACID LINKERS

WANNUR SOFIASALAMAH KHAIRIAH AB RAHMAN

FACULTY OF SCIENCE
UNIVERSITY OF MALAYA
KUALA LUMPUR

2017

STRUCTURAL STUDIES OF SELF-ASSEMBLED Cu(II), Ni(II) AND Cd(II) COORDINATION POLYMERS FABRICATED WITH AMINE LIGANDS AND DICARBOXYLIC ACID LINKERS

WANNUR SOFIASALAMAH KHAIRIAH AB RAHMAN

DISSERTATION SUBMITTED IN FULFILMENT OF THE REQUIREMENTS FOR THE MASTER DEGREE OF SCIENCE

DEPARTMENT OF CHEMISTRY
FACULTY OF SCIENCE
UNIVERSITY OF MALAYA
KUALA LUMPUR

2017

UNIVERSITY OF MALAYA

ORIGINAL LITERARY WORK DECLARATION

Name of Candidate: Wannur Sofiasalamah Khairiah Ab Rahman

Registration/Matric No: SGR130053

Name of Degree: Master of Science

Title of Project Paper/Research Report/Dissertation/Thesis ("this Work"):

Structural Studies of Self-Assembled Cu(II), Ni(II) and Cd(II) Coordination Polymers Fabricated with Amine Ligands and Dicarboxylic Acid Linkers

Field of Study: Inorganic Chemistry

I do solemnly and sincerely declare that:

(1) I am the sole author/writer of this Work;
(2) This Work is original;
(3) Any use of any work in which copyright exists was done by way of fair dealing and for permitted purposes and any excerpt or extract from, or reference to or reproduction of any copyright work has been disclosed expressly and sufficiently and the title of the Work and its authorship have been acknowledged in this Work;
(4) I do not have any actual knowledge nor do I ought reasonably to know that the making of this work constitutes an infringement of any copyright work;
(5) I hereby assign all and every rights in the copyright to this Work to the University of Malaya ("UM"), who henceforth shall be owner of the copyright in this Work and that any reproduction or use in any form or by any means whatsoever is prohibited without the written consent of UM having been first had and obtained;
(6) I am fully aware that if in the course of making this Work I have infringed any copyright whether intentionally or otherwise, I may be subject to legal action or any other action as may be determined by UM.

Candidate's Signature Date:

Subscribed and solemnly declared before,

Witness's Signature Date:

Name:

Designation:

ABSTRACT

Self-assembly process of Cu(II), Ni(II) and Cd(II) metal ions using ethylenediamine (en) or o-phenylenediamine (o-phen) ligands with adipic (**L1**) or teraphtalic acid (**L2**) linkers respectively in solution resulted unexpected coordination polymers and one dimeric complex. A total of seven crystals were successfully obtained; $[Cu(en)(L1)]\cdot L1H_2$ **(1)**, $[Cu(en)(L2)(H_2O)_2]$ **(2)**, $[Ni(en)(L1)(H_2O)_2]\cdot H_2O$ **(3)**, $[Ni(o\text{-}phen)_2(L2)]$ **(4)**, $Ni_2(en)_2(L2)_2(H_2O)]$ **(5)**, $[Cd(en)(L2)(H_2O)]$ **(6)**, and $[Cd_2(o\text{-}phen)_2(L1)(Cl)_2(H_2O)_2]$ **(7)** showing different molecular structures and crystal packing. Structural studies revealed the incorporation of the different carboxylate moiety as linkers which led to 1-dimensional zig-zag chains for **1** and **2**, 1-dimensional linear chains for **3** and **4**, 3-dimensional chains for **5**, 2-dimensional chains for **6** with a dimeric molecular structure for **7**. The series outlined the principle of crystal engineering and supramolecular chemistry where crystal structures are always unpredictable. All structures were dominated by the persistent hydrogen bonding as the primary synthon. The coordination entity also were confirmed by using IR spectroscopy. PXRD patterns showed consistency between the bulk materials with the calculated pattern generated using SCXRD data.

ABSTRAK

Proses penyusunan sendiri dan suai padan ion logam Cu (II), Ni (II) dan Cd (II) menggunakan ligan etilenediamina (en) atau o-fenilendiamina (o-phen) dengan asid adipik (L1) atau teraftalik (L2) sebagai penghubung, masing-masing dalam larutan menghasilkan polimer koordinatan yang tidak dijangka dan satu komplek dimerik. Sebanyak tujuh hablur telah berjaya diperolehi; $[Cu(en)(L1)]\cdot L1H_2$ (**1**), $[Cu(en)(L2)(H2O)_2]$ (**2**), $[Ni(en)(L1)(H_2O)_2]\cdot H_2O$ (**3**) , $[Ni(o\text{-}phen)_2(L2)]$ (**4**), $Ni_2(en)_2(L2)_2(H_2O)]$ (**5**), $[Cd(en)(L2)(H_2O)]$ (**6**), dan $[Cd_2(o\text{-}phen)_2(L1)(Cl)_2(H_2O)_2]$ (**7**) di mana semuanya menunjukkan struktur molekul dan padatan hablur yang berbeza. Kajian struktur hablur menunjukkan bahawa hasil gabungan asid karbosilik yang berbeza sebagai penghubung telah membawa kepada rantai zig-zag 1-dimensi untuk **1** dan **2**, rantai linear 1-dimensi untuk **3** dan **4**, rantai 3-dimensi untuk **5**, rantai 2-dimensi untuk **6** dengan struktur molekul dimerik untuk **7**. Siri ini menekankan prinsip dalam bidang kejuruteraan sistem hablur dan kimia supramolekul yang mana struktur hablur adalah sentiasa tidak menentu. Semua struktur dipelopori oleh ikatan hidrogen yang kuat sebagai ikatan utama. Entiti koordinatan itu juga yang disediakan juga dapat dikenalpasti dengan menggunakan teknik spektroskopi IR. Corak PXRD menunjukkan persamaan di antara bahan pukal dengan corak yang didapati daripada data SCXRD.

ACKNOWLEDGEMENTS

Alhamdulillah, my praises all to Allah SWT for His Greatness and blessing throughout my master research. First of all, I would like to express my highest gratitude to my supervisor Dr. Siti Nadiah binti Abdul Halim and my co-supervisor Prof Dr. Hapipah Mohd Ali for their continuous guidance, encouragement, and constructive criticism in order for me to complete my master research. Many thanks also to Dr.Afzal for his guidance (dye studies).

I sincerely would like to thanks my fellow lab mates (Artikah, Izzati, Jimmy, Sherin and Kak Shimar) and fellow friends (Kak Thirah, Suhaila, Farha, Suba, Hameme, Liza, Suhaila Ramli, Rohani) for being with me all these years. All the advices, help and encouragement from all of you would not be forgotten. Not to be forgotten, many thanks to my family especially my late father, my beloved mother, Pn. Dyg Sa'diah binti Abg Masagus for giving me support, encouragement, happiness when I'm feeling down, and never ending love all this while. I would not be who I am without all of you. Thank you for being there during my hardest and happiest moments all this while.

Thanks to all for your kind contributions in any way.

TABLE OF CONTENTS

LIST OF FIGURES

LIST OF SCHEMES

LIST OF TABLES

LIST OF SYMBOLS AND ABBREVIATIONS

%	:	percentage
°C	:	degree Celsius
ml	:	milliliter
mmol	:	millimoles
CSD	:	Cambridge Structural Database
FT-IR	:	Fourier Transform Infrared
CHN	:	Carbon, Hydrogen, Nitrogen
PXRD	:	Powder X-Ray Diffraction
SCXRD	:	Single Crystal X-Ray Diffraction
MeOH	:	Methanol
DMF	:	Dimethylformamide
en	:	ethylenediamine
o-phen	:	o-phenylenediamine
L1	:	Adipic acid
L2	:	Terephthalic acid
1	:	$[Cu(en)(L1)]\cdot L1H_2$
2	:	$[Cu(en)(L2)(H_2O)_2]$
3	:	$[Ni(en)(L1)(H_2O)_2]\cdot H_2O$
4	:	$[Ni(o\text{-}phen)_2(L2)]$
5	:	$[Ni_2(en)_2(L2)_2(H_2O)]$
6	:	$[Cd(en)(L2)(H_2O)]$
7	:	$[Cd_2(o\text{-}phen)_2(L1)(Cl)_2(H_2O)_2]$
SPA	:	Solid Phase Adsorption
CSB	:	Chicago Sky Blue

CHAPTER 1: INTRODUCTION AND LITERATURE REVIEW

1.1 Crystal Engineering and Supramolecular Chemistry

The area of crystal engineering is currently expanding and has brought together researchers from a variety of disciplines. The concept of crystal engineering was introduced by Pepinsky in 1955 (Braga *et al.*, 2003) and the term was further described by Schmidt in 1971 in connection with his photodimerisation reaction of crystalline cinnamic acids (Schmidt, 1971). Later in 1989, Desiraju defined crystal engineering as *"…the understanding of intermolecular interactions in the content of crystal packing and in the utilization of such understanding in the design of new solids with desired physical and chemical properties"* (Desiraju, 1989). According to him, there were three distinct activities in crystal engineering, which formed continuous sequences: 1) the study of intermolecular interactions; 2) the study of packing modes, in the context of these interactions and with the aim of defining a design strategy; and 3) the study of crystal properties and their fine-tuning with deliberate variations in the packing. These three stages represent the "what", "how", and "why" of crystal engineering (Desiraju, 2007). Brammer considered crystal engineering as "the design and synthesis of crystalline materials through the self-assembly of molecular building blocks", where main objective was the development of new crystalline materials with variety of properties, functions and applications (Brammer *et al.*, 2004).

Since crystal engineering highlighted the idea of designing and synthesizing solid state structures, the choice of molecules to be assembled in order for the interactions to happen or the 'building blocks' are important. Therefore, crystal engineering shows reciprocal relations with the area of supramolecular chemistry. Supramolecular chemistry is defined as 'chemistry beyond the molecule', *i.e.* bearing on the organized entities of higher complexity that result from the association of two or more chemical species held together by the intermolecular forces pioneered by Jean-Marie Lehn in 1988. The chemistry of

molecular aggregates assembled *via* non-covalent interactions involved in order to form the supramolecular entities (Lehn, 1988). Dunitz later expressed that "a supermolecule *par* excellence", is an assembly of literally millions of molecules self-crafted by mutual recognition at an "amazing level of precision (Dunitz, 1991). This can be explained by indicating that if covalent bonds connected the atoms to build molecules, the intermolecular interactions connect the molecules to form the solid-state supermolecules (crystals). Supramolecular chemistry describes compounds as the composed of two or more molecules or ions that are held together in unique structural relationships by forces other than those of full covalent bonds, which encompasses the idea of molecular recognition and interactions through the noncovalent bonding: hydrogen and ionic bonds, van der Waals forces and hydrophobic interactions as an extension to the previous history introduced Lehn and Dunitz. **Figure 1.1** shows the general overview of the molecular recognition of molecules to give supermolecules to form crystal.

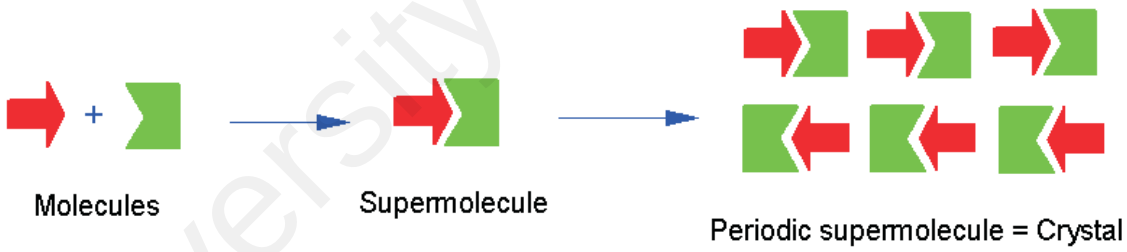

Figure 1.1: Molecular recognition of molecules to produce supermolecule and the periodic arrangement of supermolecules in a crystal lattice. (Nangia, 2010)

As these two sub-areas in chemistry overlap, terminologies used in both areas are very similar. In order to design the molecular solid state structure with desired properties, the building blocks used are known as tectons. The tectons are expected to interact with each other to achieve organization of molecules through the molecular recognition process *via* the functional groups embedded within the molecule. Tectons can exist as neutral or charged species which can be either organic or inorganic compounds. Therefore, the

combinations either neutral or charged organic-organic, inorganic-inorganic, and organic-organic tectons are possible to create new compounds (Fournier *et al.*, 2003; Planeix *et al.*, 2003).

The tectons are expected to interact with each other to achieve the organization of molecules through the molecular recognition process or self-assembly in the solid-state. As discussed earlier, the crystal engineering and supramolecular chemistry include the studies of intermolecular interaction known as synthons. The term "synthon" was introduced by Corey which was defined as, "*a structural unit within a molecule which is related to a possible synthetic operation"* (Corey, 1967). Synthons include hydrogen and halogen bondings, π-π interaction and other secondary bonding which also include electrostatic interactions.

a) Homosynthon b) Heterosynthon

Figure 1.2: Schematic representation of complementary hydrogen-bonded supramolecular homo- and heterosynthons: a) composed of two carboxylic acid moieties to form dimer; b) composed of carboxylic acid and amide moieties. (Bis & Zaworotko, 2005)

There are two types of synthons; supramolecular homosynthon (composed of self-complementary functional groups, as illustrated by the carboxylic acid dimer) and supramolecular heterosynthon (Bis & Zaworotko, 2005) (composed of different but complementary functional groups) as shown in **Figure 1.2**.

Most reported structures in crystal engineering and supramolecular chemistry discussed hydrogen bonds as synthons. Etter introduced the graph sets based on the graph theory for classifying hydrogen bond patterns into simpler notations. A graph set is denoted as

$$G_d^a[r]$$

Where '*G'* is a pattern designator, '*r'* is its degree, '*d*'denotes the number of donors and '*a' is* the number of acceptors. The pattern designator has four different assignments: *S, C, R,* and *D* based on whether hydrogen bonds are inter- or intramolecular. *S* (self) denotes an intramolecular hydrogen bond whereas for the intermolecular bonds, *C* refers to the hydrogen-bonded infinite chains, *R* refers to rings and *D* refers to the non-cyclic dimers and other finite hydrogen bonded sets (Etter, MacDonald, Bernstein, & IUCr, 1990). For instance, an acid dimer (homosynthon) and the acid-amide dimer (heterosynthon) as shown in **Figure 1.2** (a and b) are represented using the $R_2^2[8]$ graph set.

Repeating synthons are known as motifs. These motifs were found to create one-, two- and three-dimensional structures. The studies were expended to the area of co-crystal, crystalline salts, coordination polymers (CPs), and metal-organic frameworks (MOFs) later on. **Figure 1.3** shows the tentative hierarchies of CPs and MOFs. These two terminologies often overlap with each other, thus, a project was initiated by the IUPAC division of Inorganic Chemistry to give guidelines and better understanding (Batten *et al.*, 2012).

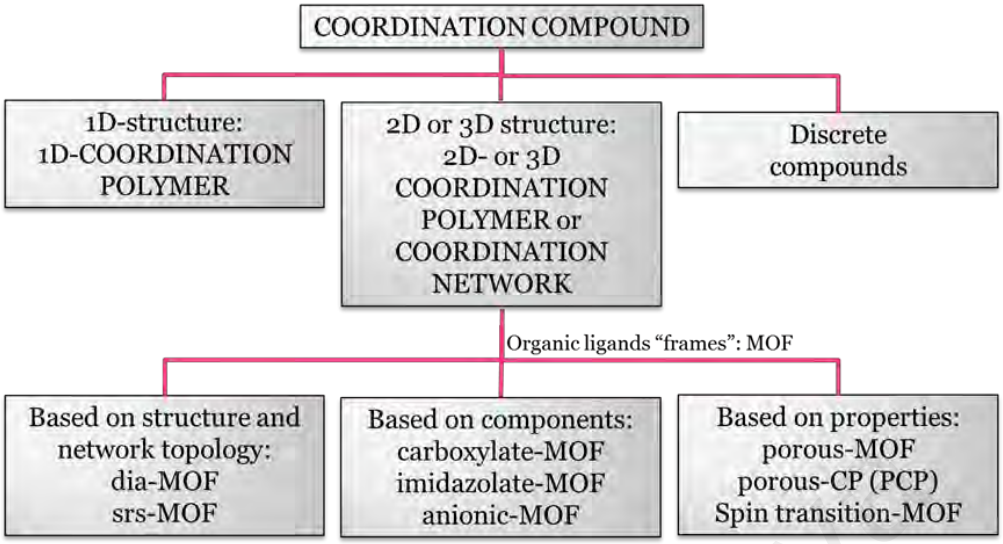

Figure 1.3: Tentative hierarchy of coordination polymers and the metal organic framework. (Batten *et al.*, 2012)

1.2 Coordination Polymers

Coordination polymers (CPs) are infinite systems that consist of metal ions and organic ligands (**Figure 1.4**). The area of coordination polymers combined the knowledge of coordination chemistry; having a coordination compound displaying polymeric arrangements (Choi, 2010; Kukovec *et al.*, 2011; Wen *et al.*, 2010). This terminology described "a coordination compound with repeating coordination entities extended in 1, 2, or 3 dimensions" and showed polymeric structures, according to the IUPAC 2013 Recommendations (Batten *et al.*, 2013). The term coordination polymer was first used by Shibata in 1916 to describe the dimers and trimers of various cobalt(II) ammine nitrates and has been continuously used in the scientific literature (Shibata, 1916).

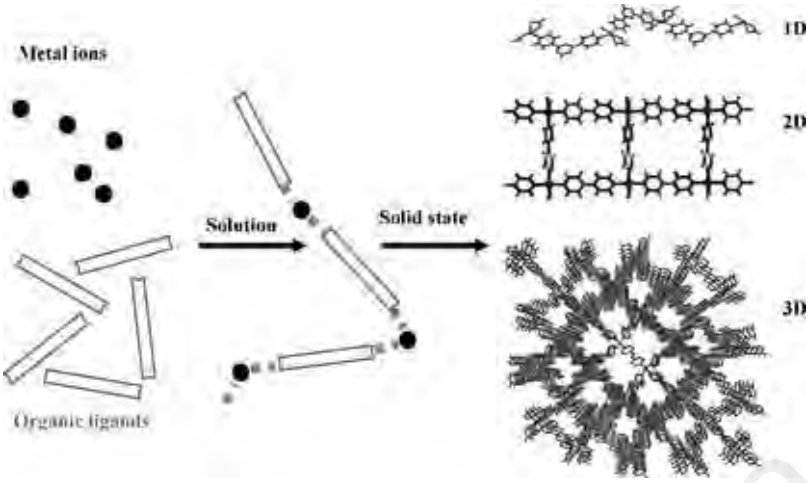

Figure 1.4: Formation of coordination polymers. (Robin & Fromm, 2006)

The area of CPs has been explored by researchers recently due to their interest in the molecular topologies (**Figure 1.5**) as well as potential applications as functional materials for their luminescence, magnetism and also their thermal properties (Bisht *et al.*, 2014; Li *et al.*, 2001; B. Liu *et al.*, 2013; X. Liu *et al.*, 2008; Okubo *et al.*, 2013; X. L. Wang *et al.*, 2009; Yan *et al.*, 2012). The synthesis of CPs embedded two different organic entities which can be of the same ligand or two different ligands; one can be a ligand and the other as linkers (Bai *et al.*, 2011). The self-assembly process presented difficulties in predicting the structures exactly, thus, the best strategy was to employ appropriate ligand as a spacer to bind with the metal centre in different modes, resulting in new CPs with different architectures (Jin *et al.*, 2012; Sun *et al.*, 2001; Zhang *et al.*, 2015). Therefore, the area of coordination polymer has overlapped with the area of metal organic framework (MOFs).

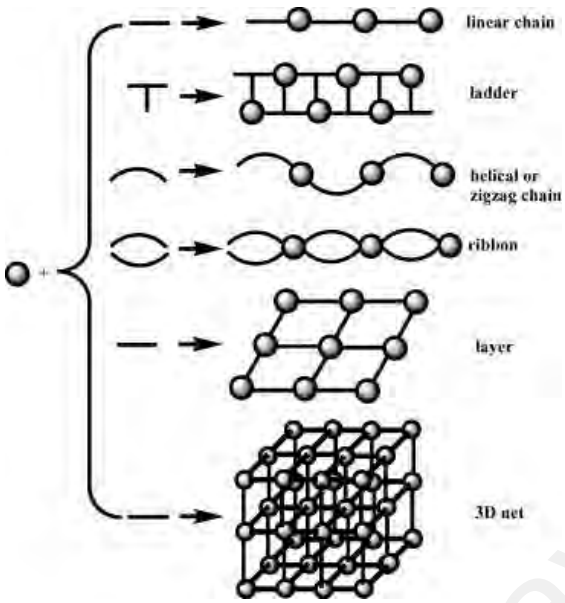

Figure 1.5: Topologies of some CPs. (Ye, Tong, & Chen, 2005)

1.3 Carboxylate coordination polymers

The crystal engineering of CPs and MOFs usually are designed to give porous structure which can have possible application such as in gas storage and adsorption studies. The ideas to incorporate dicarboxylate as linkers in CPs have been inspired researchers which can be seen from numerous reports in the literature. 1,4-benzenedicarboxylate/terephthalate has been studied extensively due to its rigidity, which was used in the well-known MOF-5, as reported by Yaghi *et al.* (1999). In this structure, the Zn_4O groups were linked by terephthalate = 1,4-benzenedicarboxylate(BDC) to form a neutral framework of $Zn_4O(BDC)_3$ composition. This material had large pores (shown as a yellow ball in **Figure 1.6**) which were filled with solvent. The area could be readily emptied thus had an unprecedentedly large surface area. Large quantities of gases such as nitrogen and methane could reversibly be absorbed to the empty area which indicated one of the example of the gas storage application of the MOFs. It also had excellent thermal stability. *B*ased on the same net topology, these series of compounds were then developed by Eddaoudi *et al.* by replacing

the terephthalate by other dicarboxylate linkers (Eddaoudi *et al.*, 2002) and known as *isoreticular*.

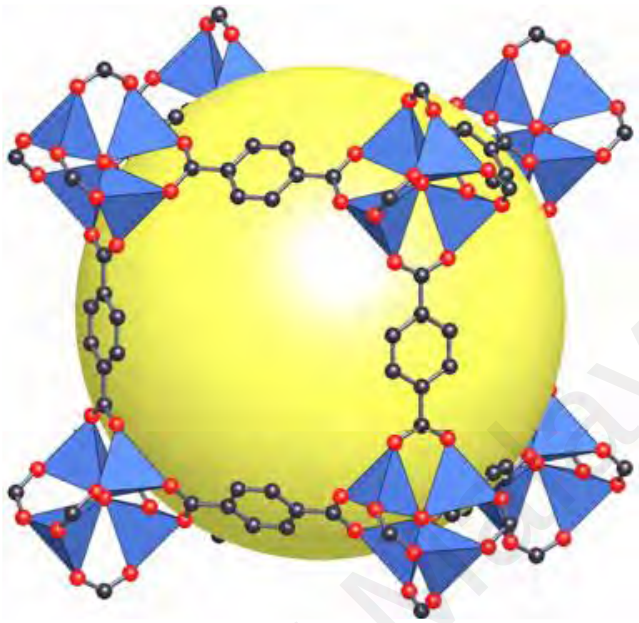

Figure 1.6: A fragment of the structure of MOF-5. ZnO_4 tetrahedra are shown in blue. Carbon atoms are black and oxygen atoms are red. (Yaghi *et al.*, 1999)

In 2008, a paper on the topological diversity of coordination polymers containing the rigid terephthalate and a flexible n,n′-type ligand was published by Wang and co-workers (G. H. Wang *et al.*, 2008). This paper highlighted the effects of the ligands and metal salts on structural motif which resulted in four coordination polymers of Zn(II) and Cd(II) synthesized with terephthalic acid (H_2tp) and 1,3-bis(4-pyridyl)propane (bpp); $[Zn(\mu\text{-tp})(\mu\text{-bpp})]_n \cdot 2nH_2O$ (**I**), $[Cd_2(\mu\text{-tp})2(\mu\text{-bpp})3]_n \cdot 2nH_2O$ (**II**), $[Cd(\mu\text{-tp})(\mu\text{-bpp})(H_2O)]_n \cdot nH_2O$ (**III**), and $[Cd_2(\mu\text{-tp})(\mu\text{-bpp})_2(bpp)2Br_2]_n$ (**IV**). Different structural motifs can be seen from the reaction of tp and bpp ligands with different metal salt. One of the motif was two interlocked sets of honeycomblike sheets of **III** which consist of Cd metal ion are shown in **Figure 1.7**.

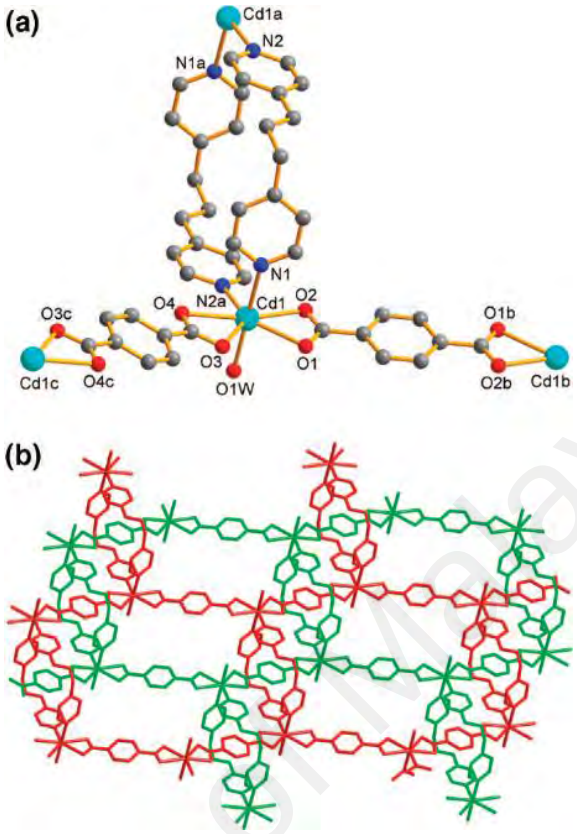

Figure 1.7: (a) Coordination environment of the Cd(II) atom in III. (b) Two interlocked sets of honeycomblike sheets. (G. H. Wang *et al.*, 2008)

The effect of the flexibility (the spacer length of carboxyl groups and the structural rigidity of the spacer) of organic dicarboxylate ligands have been investigated by Wang *et al*. in 2009 using two aromatic dicarboxylic acid ligands; biphenylethene-4,4'-dicarboxylic acid (bpea) and benzene-1,4 - dicarboxylic acid (1,4-H_2bdc). Thus, two novel metal–organic coordination polymers; [Cu(PIP)(bpea)(H_2O)]·H_2O(**CuI**) and [Cu(PIP)(1,4-bdc)] (**CuII**) have been obtained from hydrothermal reaction of copper(II) with the mixed ligands bpea for **CuI**, 1,4-H_2bdc for **CuII**, and [2-phenyl- imidazo[4,5-f]1,10-phenanthroline (PIP)] (X. L. Wang *et al.*, 2009).

Transition metals and carboxylates usually lead to a variety of secondary building units (SBUs) which can influence the final structure. Wang and co-workers recently reported the three 2D Cd(II) coordination polymers in which $Cd(NO_3)_2 \cdot 4H_2O$ was solvothermally assembled with three aromatic dicarboxylic acids; $[Cd_3(tpa)_3(DMA)_4]$ (Cd**I**), $[Cd_2(thpa)_2(DMA)_2 \cdot DMA]$ (Cd**II**), and $[Cd_3(eba)_3(DMA)]$ (Cd**III**) (H_2tpa = terephthalic acid, H_2thpa = thiophenedicarboxylic acid, H_2eba = (ethene-1,2-diyl)dibenzoic acid, DMA = N,N′-dimethylacetamide). The CPs showed different networks based on various secondary building units (SBUs); $[Cd_3(COO)_6]$ and $[Cd_4(COO)_8]$. Cd**I** (**Figure 1.8**) and Cd**III** compound exhibited a 2D six-connected hxl (hxl = hexagonal lattice) network based on hourglass-like $[Cd_3(COO)_6]$ SBUs whereas Cd**II** displays a 2D 4^4-sql (sql = square lattice) network based on $[Cd_4(COO)_8]$ SBUs. (X.P. Wang *et al.*, 2016).

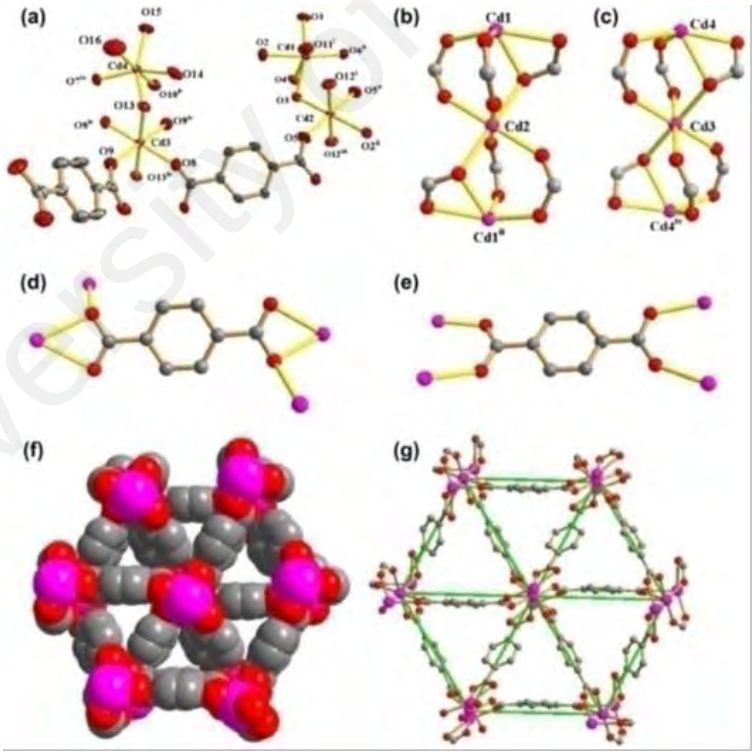

Figure 1.8: (a) Coordination environments of Cd(II) in CdI with the thermal ellipsoids at 50% probability level. (b) and (c) Ball-and-stick representation of the 6-connected $[Cd_3(COO)_6]$ SBU. (d) and (e) Coordination modes of the H_2tpa ligand. (f) The space-filling and (g) Ball and-stick view of hxl net in CdI. (X. P. Wang *et al.*, 2016)

Different from the rigid dicarboxylate spacer ligands, conformational and coordination versatility were displayed by the saturated aliphatic dicarboxylate ligands due to single-bonded carbon chains and are viewed as important flexible spacer ligands. Li and co-workers reported two porous network; $[Cu_2(malonato)_2(bipy)(H_2O)_2]\cdot H_2O$ and $[Cd(malonato)(py)(H_2O)]$ bearing both flexible and rigid ligands. They investigate the parameters contributing to the assembly of materials from different molecular building blocks, aiming at constructing porous polymers by co-assembling both rigid (4,4'-bipyridine or pyridine) and flexible (malonate anion) ligands with transition metal ions (J.-M. Li *et al.*, 2000) which resulted in two-dimensional square network possessing two kind of squares of Cu complex and two-dimensional sheet structure for the Cd complex.

In 2011, the generation of a series of coordination polymers whose two-dimensional and three-dimensional topologies depend on coordination environment, adipate conformation and carboxylate binding mode, and piperazinyl ring protonation.was reported by Banisafar and co-workers by hydrothermal reaction of divalent metal salts(Cd, Cu, Co and Ni), adipic acid and bis(4-pyridylmethyl)piperazine (bpmp) (Banisafar *et al.*, 2011). The dipyridyl ligand can provide structure-directing hydrogen-bonding points of contact or protonation sites at its piperazinyl nitrogen atoms and expected to provide different topologies.

All literature review mentioned earlier have been focusing on dicarboxylate as one of the linker/ligands. We can see that selection of ligand with variable substituents, geometries, and coordination sites is tremendously important because changing the structures of the ligands can influence the final networks. The papers provided several strategies in order to synthesis CPs/MOF. As of Yaghi works mainly focused on porous structure of MOF, the rigidity of the terephthalate, flexibility of adipate and n,n′-type

ligand also played important factor in constructing and synthesized different topological structures as discussed earlier. Thus, we are interested to study on the self-assembled of metal ions with terephthalate and adipate as linker, as well as fabricating simple amine as ligand. Most of the reported structures undergo hydrothermal and solvothermal reaction but this project highlight on the self-assembly process where all the metal ion, ligands and linkers were given the freedom to bind and form 3-D structures.

1.4 Application: Dye adsorption studies

The design and synthesis of different types of MOFs/coordination polymer for the removal of dyes also have become an interesting area and been reported in many literatures (Ai *et al.,* 2014; Du et *al.*, 2011; Van de Voorde *et al.*, 2014; Zhao *et al.*, 2015). In 2010, Haque and co-workers reported on the adsorptive removal of methyl orange (MO), a harmful anionic dye, from aqueous solutions by two typical highly porous metal-organic framework (MOF) materials based on chromiumbenzenedicarboxylates (Cr-BDC) obtained from Material of Institute Lavoisier with special structure of MIL-101 and MIL-53. The adsorption capacity and adsorption kinetic constant of MIL-101 are greater than those of MIL-53, showing the importance of porosity and pore size for the adsorption (Haque *et al.*, 2010). Later on, an iron terephthalate (MOF-235), has been used for the removal of methyl orange (MO) and methylene blue (MB) from contaminated water also via adsorption. The adsorption capacities of MOF-235 are much higher than those of an activated carbon (Haque, Jun, & Jhung, 2011). Therefore, we decided to do preliminary test of the samples prepared in this thesis for dye adsorption studies.

1.5 Research Project and Objectives

This research study is on the mixed-ligand coordination polymers where the common ethylenediamine (en) and *o*-phenylenediamine (*o*-phen) were used as the ligands in combination with Cu(II), Ni(II) and Cd(II) metal ions. The classical coordination compound then will be introduced with a dicarboxylate linker. Thus, we chose terephthalate (L2), with versatile modes of coordination, and adipate (L2) as the linkers for the design and construction of the metal-organic coordination polymers which are expected to exhibit various topological structures as discussed in the literature review. Herein we report seven different CPs formed upon the self-assembly and molecular recognition process constructed from dicarboxylate linkers L1 or L2 with the classical ethylenediamine (en) or *o*-phenylenediamine (*o*-phen) ligands as displayed in **Scheme 1.1** and **Scheme 1.2**.

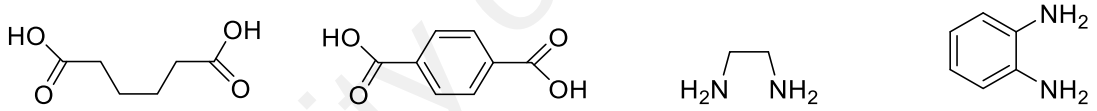

Adipic acid (L1) Terephtalic acid (L2) en *o*-phen

Scheme 1.1: Structures of amine ligands and dicarboxylate linkers used in this work.

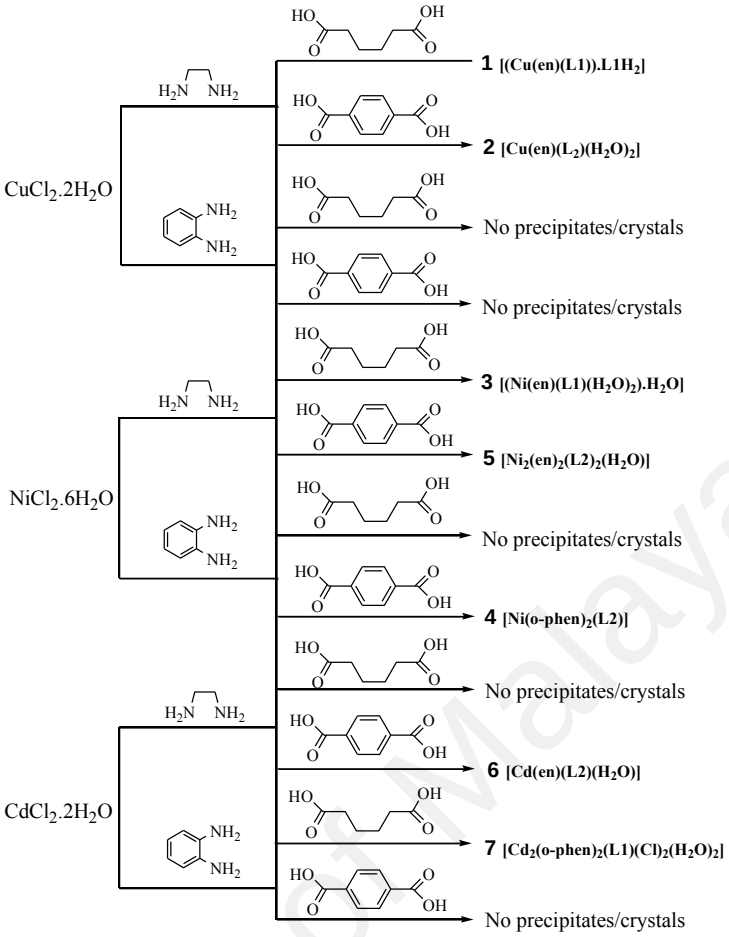

Scheme 1.2: Synthetic pathway of dicarboxylic coordination polymers.

Therefore, the objectives of this research were as follows:

(a) To evaluate the self-assembly process of metal ions, amine ligands, and carboxylate linkers in the solid state; whether the self-assembly process could give rise to cation-metal complexes with carboxylate counter ions; $[M(RNH_2)][RCOO]$ or an anion-metal complexes with protonated amine counter ions; $[M(R(COO^-)_2)][\ RNH_3^+]$ or mixed ligand complexes; $[M(RNH_2)(\ R(COO^-)_2)]$.

(b) To characterize the coordination polymer complexes *via* different characterization methods; SCXRD, PXRD, FTIR and melting point.

(c) To study the structural and molecular interactions in the crystal structures of the coordinated polymers; and

(d) To test the prepared coordination polymers using dye adsorption studies.

CHAPTER 2: EXPERIMENTAL AND METHODOLOGY

2.1 Materials

All reagents and solvents used were commercially available and were used as received without further purification. The chemicals and reagents used were; $CuCl_2 \cdot 2H_2O$ (R&M Chemicals), $NiCl_2 \cdot 6H_2O$ (R&M Chemicals), $CdCl_2 \cdot H_2O$ (R&M Chemicals), ethylenediamine (Sigma), *o*-phenylenediamine (Merck), terephthalic acid (Aldrich), adipic acid (Sigma-Aldrich), methanol (R&M Chemicals), dimethylformamide (R&M Chemicals) and Chicago Sky Blue (Sigma-Aldrich) for the dye adsorption studies. The melting points were determined on a Krüss KSP1N and Mel-Temp II melting point apparatus.

2.2 Methodology

2.2.1 Synthesis of 1 [Cu(en)(L1)]· $L1H_2$

2.4040 g, 4 mmol of ethylenediamine was slowly added to an aqueous solution of $CuCl_2.2H_2O$ (3.4090 g, 2 mmol) resulting in an aqueous deep blue solution. The mixture was left stirred for about an hour. An aqueous solution of L1 (0.2923 g, 2 mmol) in MeOH was then added into the blue solution and left for continuous stirring for about 3 hours. The resultant solution was reduced by half and left for crystallization. Blue crystals suitable for the single crystal X-ray data collection were obtained after a week by slow evaporation technique. Yield: 84.67 % (2 mmol, 0.7010 g).

2.2.2 Synthesis of 2 [Cu(en)(L2)$(H_2O)_2$]

2.4040 g, 4 mmol of ethylenediamine was slowly added to an aqueous solution of $CuCl_2.2H_2O$ (3.4090 g, 2 mmol) resulting in an aqueous deep blue solution. The mixture was left stirred for about an hour. An aqueous solution of L2 (2 mmol, 0.3323 g) in DMF was then added into the blue solution and stirred for about 3 hours. The resultant solution

was reduced and left for crystallization. Blue single crystals suitable for the single crystal X-ray data collection were obtained after about a month. Yield: 16.99 % (2 mmol, 0.1100 g).

2.2.3 Synthesis of 3 $[Ni(en)(L1)(H_2O)_2]\cdot H_2O$

0.24040 g, 4 mmol of ethylenediamine was slowly added to an aqueous solution of $NiCl_2.6H_2O$ (0.4754 g, 2 mmol), resulting in an aqueous blue solution with continuous stirring for about an hour. An aqueous solution of L1 (0.2923 g, 2 mmol) in MeOH was added with continuous stirring and stirred for about 3 hours. The resultant solution was reduced and left for crystallization. Green crystals suitable for X-ray data collection were obtained after a few weeks. Yield: 51.27 % (2 mmol, 0.3250 g).

2.2.4 Synthesis of 4 $[Ni(o\text{-}phen)_2(L2)]$

0.4324 g, 4 mmol of 1,2-diphenylenediamine was slowly added to an aqueous solution of $NiCl_2.6H_2O$ (0.4754 g, 2 mmol), resulting in an aqueous yellowish solution with continuous stirring for about an hour. An aqueous solution of L2 (0.3323 g, 2 mmol) in DMF was added with continuous stirring for about 3 hours. The resultant solution was reduced and left for crystallization. Dark brown crystals suitable for X-ray data collection were obtained after a week. Yield: 57.40 % (2 mmol, 0.5041 g).

2.2.5 Synthesis of 5 $[Ni_2(en)_2(L2)_2(H_2O)]$

0.2404 g, 4 mmol of ethylenediamine was slowly added to an aqueous solution of $NiCl_2.6H_2O$ (0.4754 g, 2 mmol), resulting in an aqueous blue solution with continuous stirring for about an hour. An aqueous solution of L2 (2 mmol, 0.3323 g) in DMF was added with continuous stirring and stirred for about 3 hours. The resultant solution was reduced and left for crystallization. Green single crystals suitable for single crystal X-ray data collection were obtained after about two months. Yield: 22.18 % (2 mmol, 0.2590 g).

2.2.6 Synthesis of 6 [Cd(en)(L2)(H_2O)]

0.2404 g, 4 mmol of ethylenediamine was slowly added to an aqueous solution of $CdCl_2.2H_2O$ (0.4026 g, 2 mmol) resulting in an aqueous colourless solution. The mixture was left for continuous stirring for about an hour. (0.3323 g, 2 mmol) of L2 in DMF was then added into the colourless mixture and left for continuous stirring for another 3 hours. The resultant solution was reduced and left for crystallization. Colourless block crystals of **1** were obtained after few weeks and analysed by single crystal X-ray diffraction analysis. Yield: 80.44 % (2 mmol, 0.7064 g).

2.2.7 Synthesis of 7 [Cd_2(o-phen)$_2$(L1)$(Cl)_2(H_2O)_2$]

0.4324 g, 4 mmol of 1,2-diphenylenediamine was slowly added to an aqueous solution of $CdCl_2.2H_2O$ (0.4026 g, 2 mmol) resulting in an aqueous yellowish solution. The mixture was left for continuous stirring for about an hour to give a yellow solution followed by the addition of L1 (0.2923 g, 2 mmol) in MeOH. The mixture then was left for continuous stirring for another 3 hours. The resultant solution was reduced and left for crystallization. Brown needle crystals of **2** were obtained after few weeks and analysed by single crystal X-ray diffraction analysis. As the yield was low, the same reaction was done and the solution was evaporated to dryness. The powder was then characterized by the powder x-ray diffraction technique. Yield: 25.75 % (2 mmol, 0.3564 g).

2.3 Instrumentations

2.3.1 CHN Analysis

The elemental analyses for carbon, hydrogen, and nitrogen were done using the Perkin Elmer CHN Analyzer 2400 Spectrophotometer analytical instrument.

2.3.2 Fourier-Transform Infrared (FT-IR) Spectroscopy

The FT-IR spectra were recorded on a GladiATR with diamond crystal plate and far-IR optics in FTIR in the frequency range of 4,000–400 cm^{-1}.

2.3.3 Single-Crystal X-ray Diffraction Analysis

The X-ray data for complex **2** was collected at 296(2) K on a Bruker AXS SMART APEX II diffractometer with a CCD area detector Mo Kα, (λ = 0.71073 Å, monochromator = graphite). High-quality crystals were chosen under a polarising microscope and mounted on a glass fibre. The data processing and absorption correction were accomplished using the APEXII software package (Bruker, 2005).

X-ray data complexes for **1**, **3**, **4**, **5**, **6,** and **7** were collected at 273, 105(8), 110(3), 293(2) K, 101 K (**6** and **7)** respectively on the Oxford Supernova Dual Wavelength diffractometer Mo Kα, (λ = 0.71073 Å). The high-quality crystals were chosen carefully under a polarising microscope and mounted on a glass fibre. The absorption correction was performed by the multi-scan method using CrysAlis PRO, with empirical absorption correction using spherical harmonics, implemented in the SCALE3 ABSPACK scaling algorithm (Oxford Diffraction, 2013).

The structures were solved by the charge-flipping method using the Superflip solution programme (Palatinus & Chapuis, 2007). Hydrogen atoms were placed in geometrically calculated positions and included in the refinement process using a riding model with U_{iso} = $1.2U_{eq}$ C(H , H) groups.

All data were refined with full matrix least-squares refinement against $|F^2|$ using the SHELXTL refinement programme (Sheldrick, 2008) and the final refinement included the atomic position for all the atoms, anisotropic thermal parameters for all the non-hydrogen atoms, and isotropic thermal parameters for all the hydrogen atoms. The Olex2 programmes (Dolomanov, Bourhis, Gildea, Howard, & Puschmann, 2009), PLATON (Spek, 2009) and Mercury (Macrae et al., 2008) were used throughout the study.

2.3.4 Powder X-ray Diffraction analysis

PXRD data were recorded with a PANalytical Empyrean XRD system with Cu $K\alpha_1$ radiation, (λ = 1.54056 Å) over a 2θ range of 5 to 40°. A slit size of 0.4785° was used. A comparison between the experimental and calculated (from CIF data) PXRD patterns was performed with X'Pert HighScore Plus (PANalytical, 2009).

2.3.5 Batch Adsorption Experiments

The spectral data were obtained with a SHIMADZU UV- 2600 Spectrophotometer by dissolving the compound in the Chicago Sky Blue dye solution (10ml) at a range of 190-800nm for adsorption studies.

The adsorption of CSB dye onto **7** was performed in batch experiments in 25 mL extraction flask under optimum conditions. Following the centrifugation, the concentration of CSB dye was determined by UV-vis spectrophotometer.

The % removal of CSB and adsorption capacity was calculated by using equation 1 and 2 as follows:

$$\% \text{ Removal} = \left(\frac{C_i - C_e}{C_i}\right) \times 100 \qquad (1)$$

Where C_i (mol L^{-1}) is the initial concentration of solution before the adsorption and C_f (mol L^{-1}) is the final concentration after the adsorption of the CSB.

$$q_e = \frac{V}{m}(C_i - C_e) \qquad (2)$$

Where Ci and Ce are the initial and equilibrium concentrations of CSB (mg L^{-1}), m is the mass of adsorbent (g) and V is volume of the solution.

For the quantitative removal of the CSB dye the solid phase adsorption (SPA) method was optimized through different factors *i.e.*, adsorbent dosage, solution pH, adsorption time and CSB concentration.

CHAPTER 3: RESULTS AND DISCUSSION

3.1 General characterization

The self-assembly and molecular recognition process gave seven new synthesised crystals which were suitable for the single crystals. The complete sets of structural parameters for the crystal **1**, **2**, **3**, **4**, **5**, **6** and **7** were deposited in the CCDC with deposition numbers 1450394, 1450395, 1450396, 1450397, 1472497, 1450393 and 1446968 respectively. Crystals **1** and **6** had high yield (84.67% and 80.44%), **3** and **4** moderate yield (51.27% and 57.40%) whereas **2, 5** and **7** gave low yield (16.99%, 22.18% and 25.75%) respectively. The low yield mentioned are the yield for crystals, which were obtained from slow evaporation method. Since they are too low, the remaining solution was evoporated to dryness to give precipitates which then were characterized with PXRD to confirm the bulk material was similar with the single crystals before it was used for further characterization. The solubility test on the crystals show that crystals **1** and **7** are soluble in a mixture of methanol and water, **2** is soluble in mixture of DMSO and water, whereas the rest are insoluble in water and common organic solvents. The complexes are air-stable with high melting point except for **1** and **3**.

The linker **L1** and **L2** on reaction with metal salts; $NiCl_2.6H_2O$, $CuCl_2.2H_2O$, $CdCl_2.2H_2O$ and amine; ethylenediamine and o-phenylenediamine, yield complexes corresponding to the general formula: **1** $[Cu(en)(L1)]\cdot L1H_2$, **2** $[Cu(en)(L2)(H_2O)_2]$, **3** $[Ni(en)(L1)(H_2O)_2]\cdot H_2O$, **4** $[Ni(o\text{-}phen)_2(L2)]$, **5** $[Ni_2(en)_2(L2)_2(H_2O)]$**,** **6** $[Cd(en)(L2)(H_2O)]$, and **7** $[Cd_2(o\text{-}phen)_2(L1)(Cl)_2(H_2O)_2]$. The elemental analysis for all compounds was conducted and the experimental values were in agreement with the calculated values.

Compound 1: [Cu(en)(L1)]·L1

Elemental analysis, Experimental (Calculated), (%): $C_{14}H_{26}Cu_1N_2O_8$: C, 40.98 (40.63); H, 6.64 (6.33); N, 7.05 (6.77). Yield: 84.67 % (2 mmol, 0.7010 g). Mp: 162.5-163.5°C.

Compound 2: [Cu(en)(L2)$(H_2O)_2$]

Elemental analysis, Experimental (Calculated), (%): $C_{10}H_{16}Cu_1N_2O_6$: C, 36.84 (37.09); H, 4.65 (4.98); N, 8.27 (8.65). Yield: 16.99 % (2 mmol, 0.1100 g). Mp: 275.5-276.5°C.

Compound 3: [Ni(en)(L1)$(H_2O)_2$]·H_2O

Elemental analysis, Experimental (Calculated), (%): $C_8H_{22}N_2Ni_1O_7$: C, 35.33 (35.86); H, 4.65 (4.82); N, 8.04 (8.36). Yield: 51.27 % (2 mmol, 0.3250 g). Mp: 137.5-138.5 °C.

Compound 4: [Ni(o-phen)$_2$(L2)]

Elemental analysis, Experimental (Calculated), (%): $C_{20}H_{20}N_4Ni_1O_4$: C, 49.35 (49.69); H, 5.20 (5.56); N, 12.59 (12.88). Yield: 57.40 % (2 mmol, 0.5041 g). Mp: 343.0-344.0 °C.

Compound 5: [Ni_2(en)$_2$(L2)$_2$(H_2O)]

Elemental analysis, Experimental (Calculated), (%): $C_{20}H_{26}Ni_1N_2O_9$: C, 40.84 (41.14); H, 4.18 (4.49); N, 9.27 (9.59). Yield: 22.18 % (2 mmol, 0.2590 g). Mp: 254.5-255.5°C.

Compound 6: [Cd(en)(L2)(H_2O)]

Elemental analysis, Experimental (Calculated), (%): $C_{10}H_{14}Cd_1N_2O_5$: C, 33.24 (33.87); H, 3.58 (3.98); N, 7.55 (7.90). Yield: 80.44 % (2 mmol, 0.7064 g). Mp: 258.0-259.0°C.

Compound 7: [Cd_2(o-phen)$_2$(L1)$(Cl)_2(H_2O)_2$]

Elemental analysis, Experimental (Calculated), (%): $C_{18}H_{28}Cd_2Cl_2N_4O_6$: C, 30.85 (31.24); H, 3.77 (4.08); N, 7.86 (8.09). Yield: 25.75 % (2 mmol, 0.3564 g). Mp: 154.0-155.0°C.

3.1.1 Infrared Spectroscopic Studies

The IR absorption bands of crystals **1**–**7** were in agreement with the absorption values of each functional groups. The absence of the absorption band at 1681 and 1673cm^{-1}, arising from the carboxylic functional group (COOH), from L1 and L2 linker. This happened upon coordination with metals, where the H atom of the COOH moiety was deprotonated to give rise to COO^- which also shifted the C-O stretch. The absorption band range of the stretching asymmetric (ν_{as}) of carboxylate group between 1525 and 1585 cm^{-1} and of the symmetric vibrations (ν_s) at 1320–1390 cm^{-1} confirmed these hypotheses (Mesubi, 1982). There were two strong bands in the range of 1300–1600 cm^{-1} when the L1 and L2 linker coordinated with metal atoms as a bridging linker. The former could be attributed to $\nu_{as}(COO^-)$, and the latter could be attributed to $\nu_s(COO^-)$. Yang *et al.* reported that if $\Delta\nu$ ($\nu_{as} - \nu_s$) > 200 cm^{-1}, carboxyl is monodentate; if Δ ($\nu_{as} - \nu_s$) < 200 cm^{-1}, carboxyl is bidentate (Yang et al., 2005). The calculated result of $\Delta\nu$ of **1**, **2**, **3**, **4**, **5**, **6**, and **7** were 196 cm^{-1}, 201 cm^{-1}, 201 cm^{-1}, 180 cm^{-1}, 200 cm^{-1}, 156 cm^{-1}, and 155 cm^{-1} respectively, which indicated the coordination of the bridging linker to the metal centre. These $\Delta\nu$ were in accordance with the crystal structure; **1** bidentate, **2** monodentate, **3** monodentate, **5** monodentate, **6** bidentate, and **7** bidentate. The $\Delta\nu$ of **4** theoretically indicated the linker is bidentate but in the crystal structure it showed that L2 linker of **4** coordinated in a monodentate manner to the the metal centre.

Table 3.1: IR stretching frequencies (cm^{-1}) of L1, L2 and their metal complexes.

Assignments	L1	L2	1	2	3	4	5	6	7
ν (H_2O)	3025	3062	-	3216	3147	-	3281	3172	3152
ν(COOH)	1681 s	1673 s	-	-	-	-	-	-	-
$\nu_{as}(COO^-)$	-	-	1583 s	1560 s	1528 s	1554 s	1577 s	1533 s	1524 s
$\nu_s(COO^-)$	-	-	1387 s	1351s	1327 m	1375 s	1377s	1377 s	1369 m
ν(C-O)	1274 m	1279 m	1290 m	1294 m	1275 m	1256 m	1282 w	1153 w	1238 w
$\Delta(\nu_{as} - \nu_s)$			196	201	201	180	200	156	155

3.2 Single Crystal X-ray Diffraction (SCXRD) Analysis

Upon the self-assembly process, suitable crystals **1**–**7** for X-ray diffraction analysis were obtained at room temperature. The selected bond lengths (Å) and angles (°) for the metal coordination centres of all crystals are presented in **Table 3.9**. The crystallographic data and structural refinement details for all crystals are presented in **Table 3.10**.

3.2.1 Crystal 1 [Cu(en)(L1)]· L1

Single crystal X-ray diffraction analysis revealed that **1** crystallized in the monoclinic crystal system with *C 2/c* space group. The asymmetric unit contained half ethylenediamine ligand, half L1 linker coordinated to one copper metal ion. A half molecule of solvated L1 linker was also observed in the asymmetric unit as displayed in **Figure 3.1**. The molecular structure is shown in **Figure 3.2** and was generated by the existence of the inversion centre and 2-fold rotational symmetry in the structure.

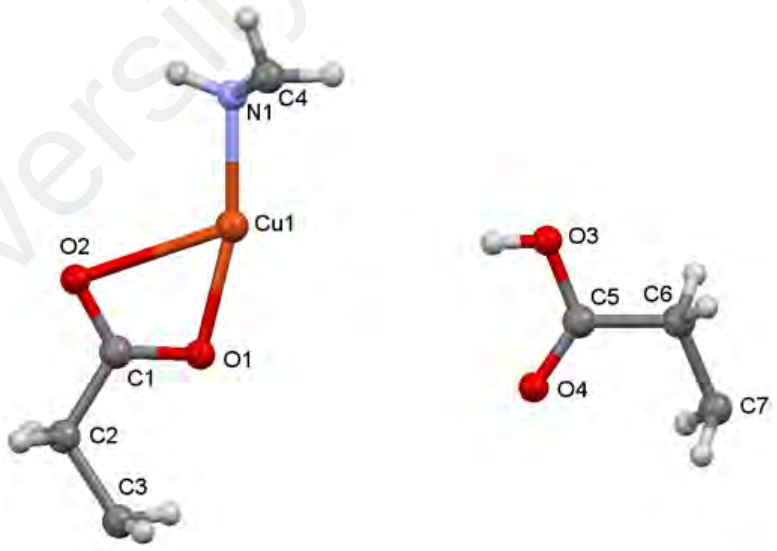

Figure 3.1: **Asymmetric unit of 1**.

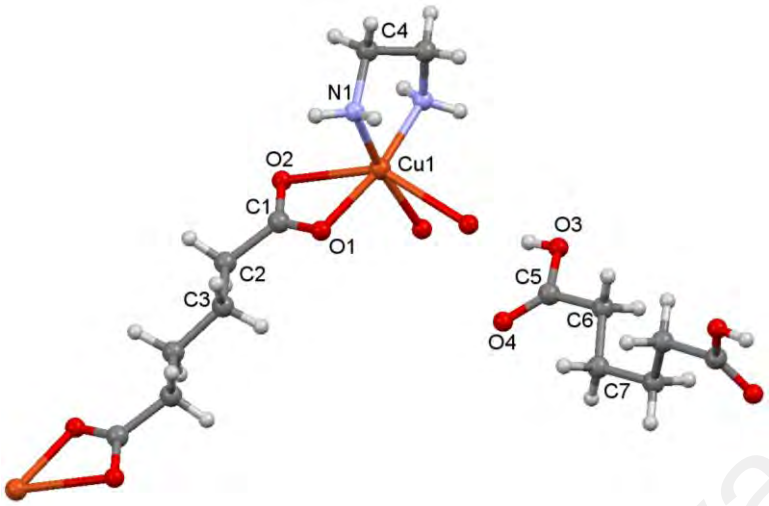

Figure 3.2: Molecular structure of 1.

The 2-fold rotation passed through the midpoint of Cu ion, coordinated ethylenediamine ligand, L1 linker (bisecting the middle of C3–C3 bond) and solvated adipic acid (bisecting the middle of C7–C7 bond). The green line and yellow dots indicate 2-fold rotation symmetry and centre of inversion respectively as shown in **Figure 3.3**.

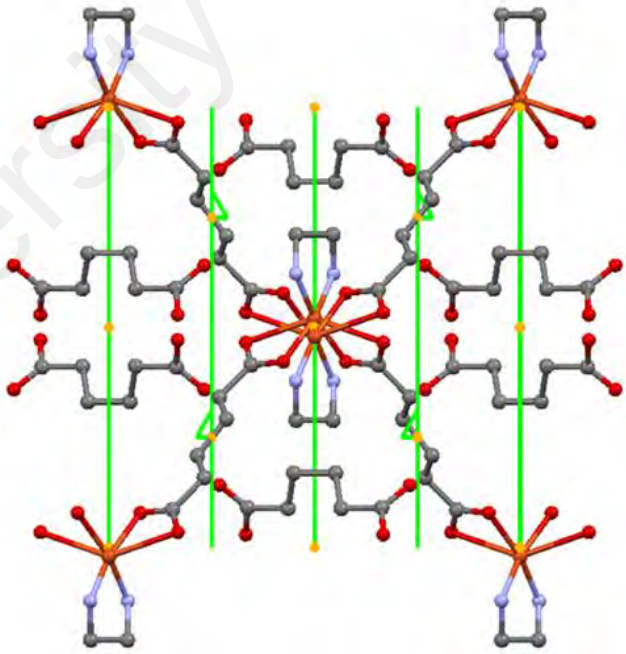

Figure 3.3: View of 2-fold rotation axis in 1 which generates other part of the structure (hydrogen atoms were omitted for clarity).

The Cu(II) ion adopts a distorted octahedral geometry, coordinated to two N atom from an ethylenediamine(Cu(1)–N(1)=1.989(11) Å), four oxygen atoms from two different bridging bidentate L1 linkers (Cu(1)–O(1)=1.994(9) Å, Cu(1)–O(2)=2.4835(10) Å).The torsion angles of the dicarboxylate linker bridging the adjacent Cu metal centres show that it is in an extended conformation with Cu···Cu separation distance of 11.002 Å. The centrosymmetric adipate made torsion angles C1–C2–C3–C3'=170.87°, C2–C3–C3'–C2=180°, C3–C2–C1–O1=8.67°, C3–C2–C1–O2=-173.15°.

Table 3.2: Hydrogen bonds in 1.

Compound 1				
D ─ H···A	**D ─ H, Å**	**H···A, Å**	**D···A, Å**	**D ─ H···A, °**
N1–H1A···O4	0.89	2.22	2.9915(14)	145
N1–H1B···O1	0.89	2.11	2.9511(14)	157
O3–H3···O2	0.82	1.76	2.5769(15)	175

Table 3.2 presents the hydrogen bonding synthons in **1**. In the structure, the coordinated nitrogen from ethylenediamine ligand N1 had hydrogen bonds to two different oxygen atoms; oxygen from the solvated L1 linker O4 (N···O distance was 2.9915(14) Å, angle N(1)–H(1A)···O(4)= 145°), and to oxygen from the coordinated L1 linker O1 (N···O distance was 2.9511(14) Å, N(1)–H(1B)···O(1)=157°) as depicted in **Figure 3.4**.

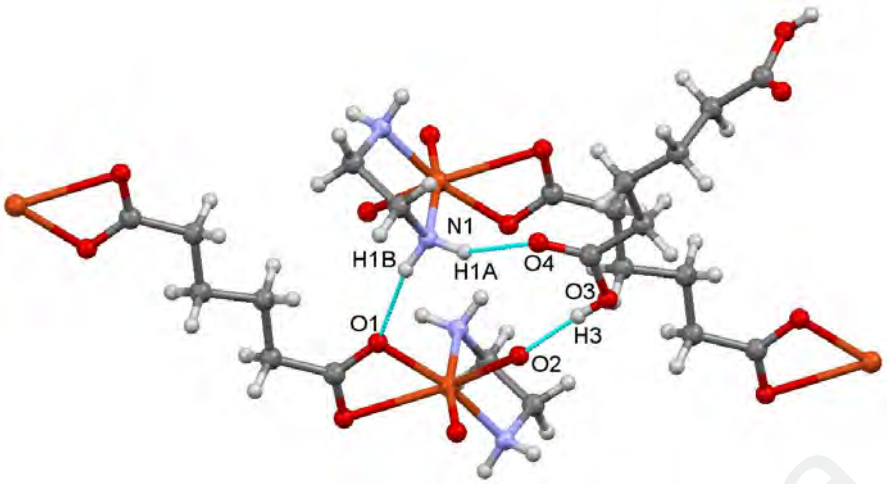

Figure 3.4 : **Hydrogen bonds environment in 1.**

The intermolecular O–H···O hydrogen bond synthon contributed by oxygen from solvated adipic acid O3 with the coordinated oxygen of L1 linker O2 (O···O distance was 2.5769(15) Å, angle O(3)–H(3)···O(4)= 175°) represented by the graph set $C_1^1[3]$ are shown in **Figure 3.5**. **Figure 3.6(a)** illustrates the packing diagram of **1** viewed along *c* showing 1-dimensional zig-zag polymeric chains**.** The repeated motifs lead to a 3-dimensional layer of **1** (**Figure 3.6(b)**).

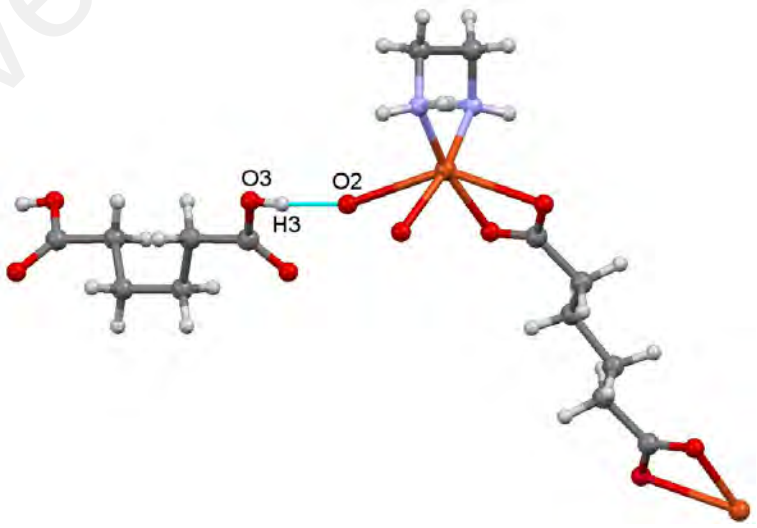

Figure 3.5: O–H···O synthon between solvated adipic acid and coordinated L1 linker.

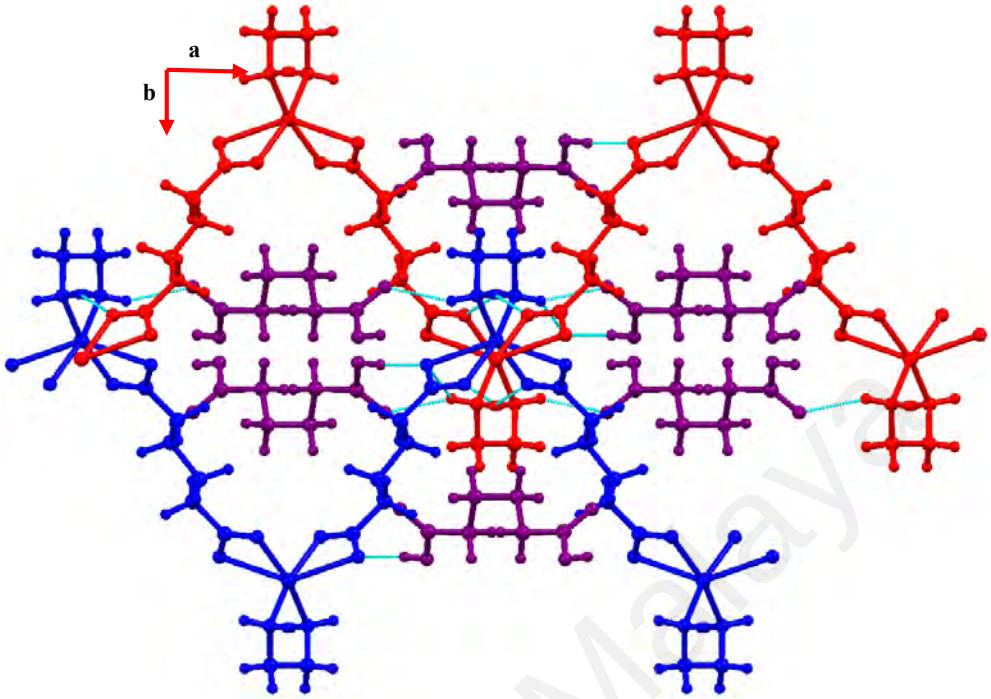

(a)

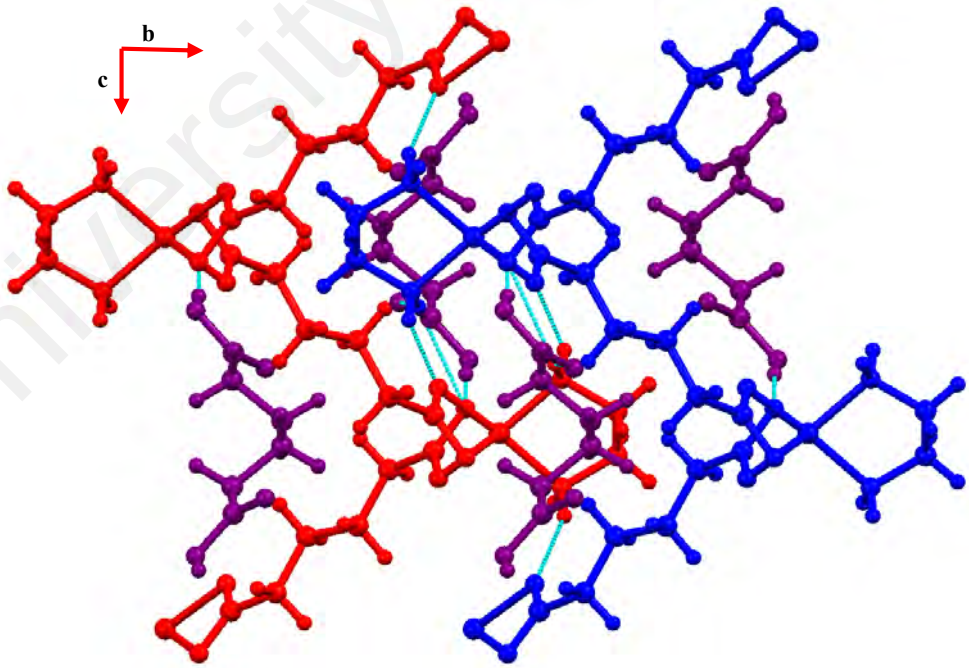

(b)

Figure 3.6: (a) Zigzag chain viewed along *c*, (b) Packing of the polymeric chain structure viewed along *a*; of 1.

Hydrogen bonds between the layers of 1-dimension polymeric chain of **1** are shown in **Figure 3.7** (solvated adipic acid was omitted for clarity). The hydrogen bond is depicted in cyan blue. Blue and red indicate different layers in the crystal packing.

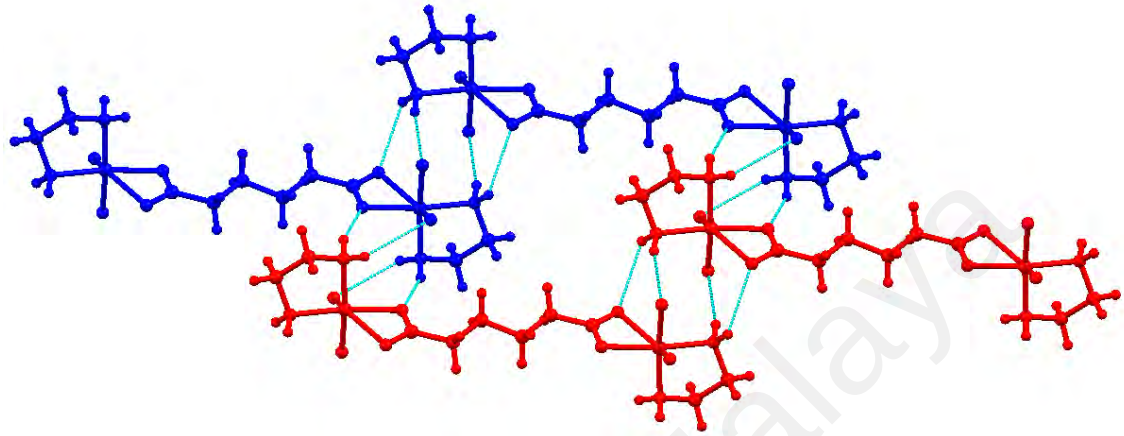

(a)

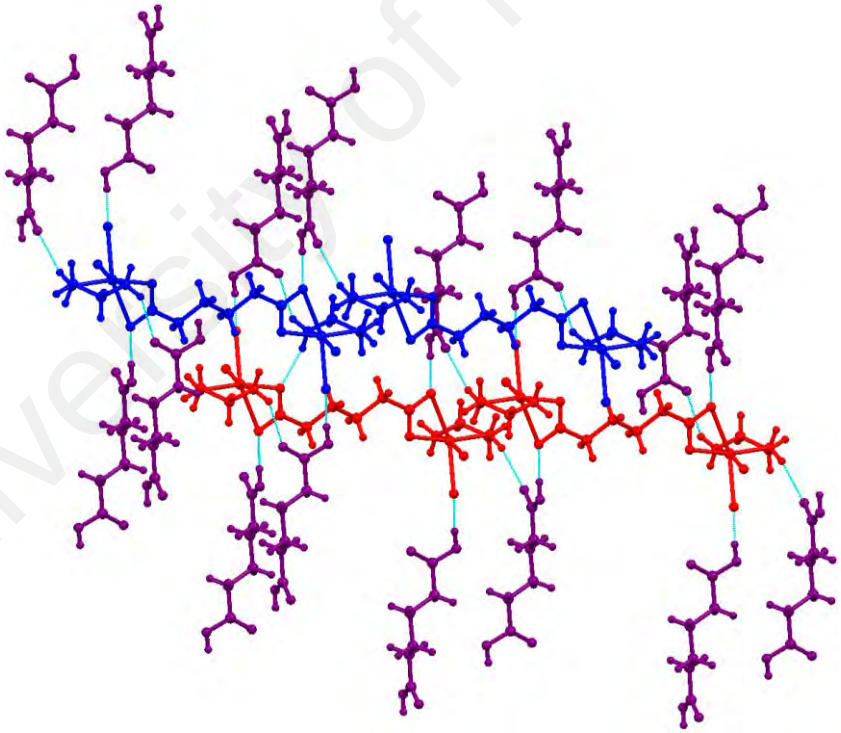

(b)

Figure 3.7: Hydrogen bonds; (a) between layers of polymeric chain and (b) between solvated adipic acid with the layers of polymeric chain leads to 1-dimensional polymeric chains. Purple: solvated adipic acid; Blue and red: different layers of polymeric chain of 1.

3.2.2 Crystal 2 [Cu(en)(L2)(H_2O)$_2$]

Single crystal X-ray diffraction analysis revealed that **2** crystallized in the monoclinic crystal system with *P 2/c* space group. The asymmetric unit contained half of one L2 linker, half of ethylenediamine ligand and one water molecule coordinated to copper metal ion as displayed in **Figure 3.8(a)**. The molecular structure shown in **Figure 3.8(b)** was generated by a 2-fold rotational symmetry (green lines) and the existence of centre of inversion (yellow dots) (**Figure 3.9).**

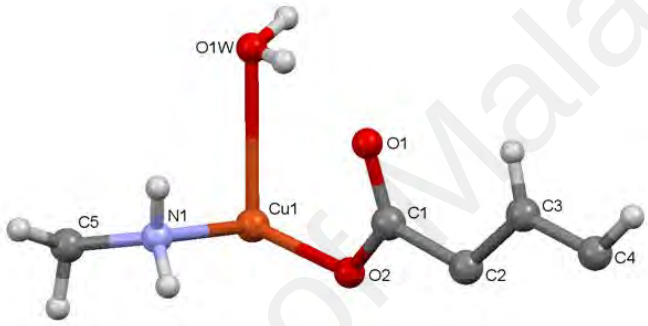

(a)

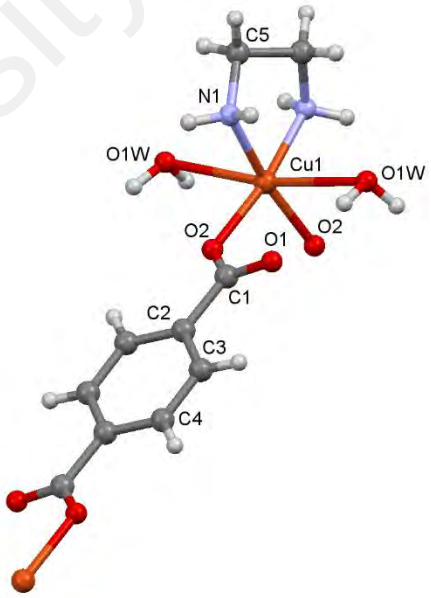

(b)

Figure 3.8: (a) Asymmetric unit and (b) molecular structure of 2.

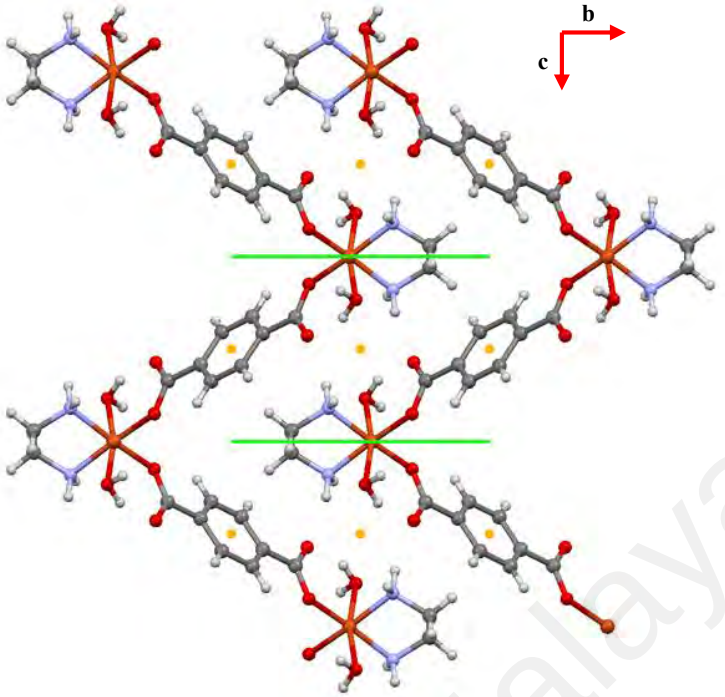

Figure 3.9: Zig zag chains of 2 viewed along *a*.

In the structure, a 2-fold rotation axis passed through the midpoint of Cu ion and C5–C5 of ethylenediamine ligand. This leads to 1-dimensional zig-zag chains viewed along *a* (**Figure 3.9**).

The metal environment can be described as a distorted octahedral in which the equatorial positions were occupied by both the ethylenediamine nitrogen donors and oxygen from different bridging monodenate L2 linker O2 and O2′ (Cu1–O2/O2′=1.955(2) Å), while the axial position is occupied by two water molecules O1w and O1w′ (Cu1–O1w/ O1w′=2.653(2) Å). The distortions from the octahedral geometry are indicated by the axial position angle of water molecule (O1w–Cu1–O1w′=170.51(12)°) and equatorial position angle of amine group and deprotonated oxygen atom from monodenate L2 linker (O2–Cu1–O2′=90.41(14)°, N1–Cu1–O2=93.22(10)°, N1′–Cu1–O2′=93.22(10)°and N1–Cu1–N1′=84.87(13)°. The four equatorial donors are not co-planar (0.171 Å), with the metal atom slightly displaced by 0.051 Å from their mean plane (**Figure 3.10**).

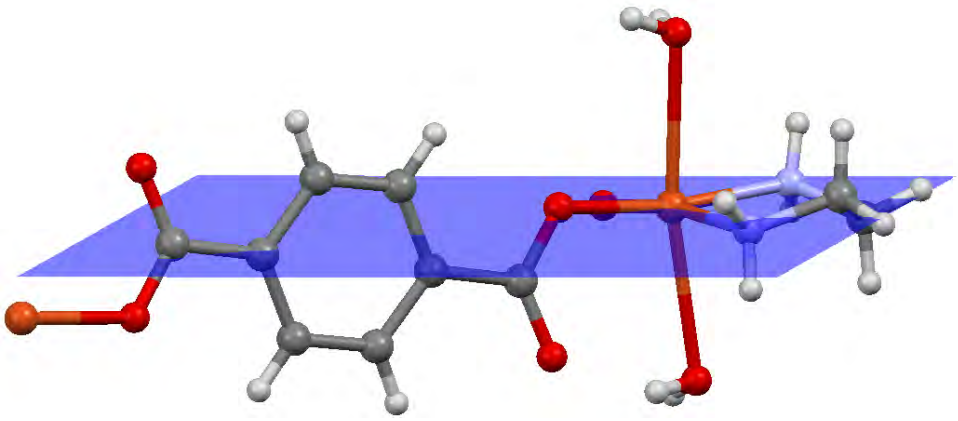

Figure 3.10: Equatorial donor atoms environment, which indicates planarity in 2.

Table 3.3: Hydrogen bonds in 2.

Compound 2				
D ─ H···A	**D ─ H, Å**	**H···A, Å**	**D···A, Å**	**D ─ H···A, °**
O1w–H1wA···O1	0.86	2.00	2.788(3)	151
N1–H1B···O1	0.89	2.18	3.051(3)	167
N1–H1A···O1w	0.89	2.23	3.077(3)	159
O1w–H1wB···O2	0.86	2.18	3.015(3)	164

Table 3.3 presents the hydrogen bonding synthons in **2.** As stated in the table, there are two hydrogen bonds initiated by nitrogen atom donor from the coordinated ethylenediamine, N1 and the other two were initiated by oxygen atom donor from the coordinated water molecule, O1w.

In the structure, one intramolecular O–H···O hydrogen bond synthon was observed between O1w with oxygen of L2 linker O1 (O···O distance was 2.788(3) Å, angle O1w–H1wA···O1= 151°) represented by the graph set $S_1^1[6]$ as shown in **Figure 3.11**. One intermolecular N–H···O synthon between nitrogen atom N1 from ethylenediamine with oxygen of L2 linker O1 (N···O distance was 3.051(3) Å, angle N1–H1B···O1=167°) contributed to $C_1^1[3]$ graph set was observed between the layers as shown in the same figure. **Figure 3.12** showed a set of $R_2^2[6]$ graph set contributed by one N–H···O synthon

connecting the nitrogen atom N1 from ethylenediamine with coordinated water molecule O1w (N···O distance was 3.077(3) Å, angle N1–H1A···O1w=159°) and one O–H···O synthon between the coordinated water molecule O1w with coordinated oxygen of L2 linker O2 (O···O distance was 3.015(3) Å, angle O1w–H1wB···O2= 164°).

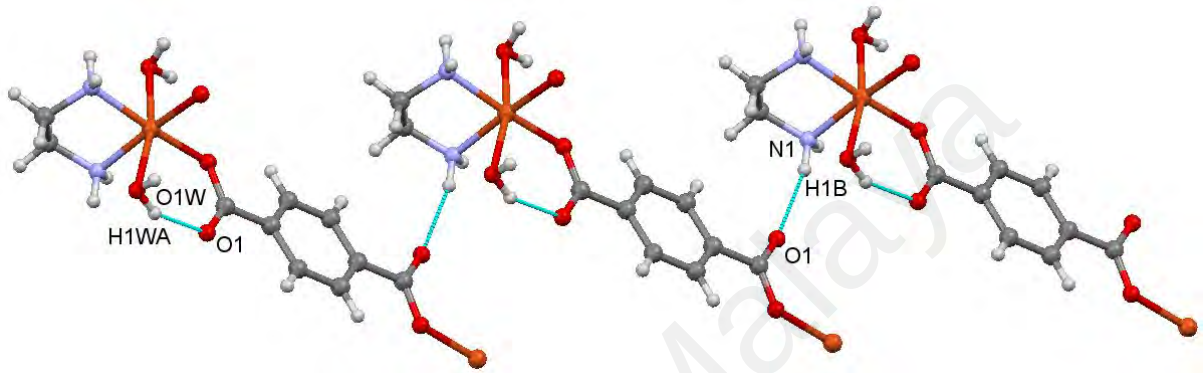

Figure 3.11: Intramolecular and intermolecular hydrogen bonds environment in 2.

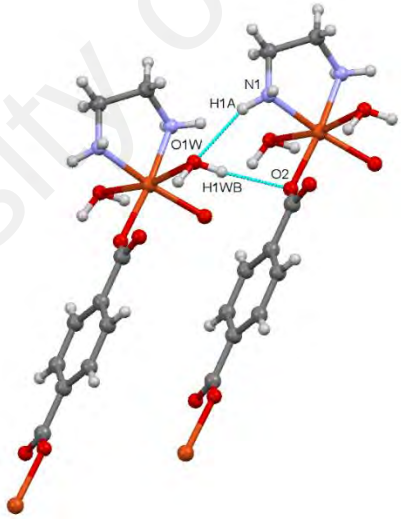

Figure 3.12: Hydrogen bond synthons in 2 connecting two different layers in the crystal packing.

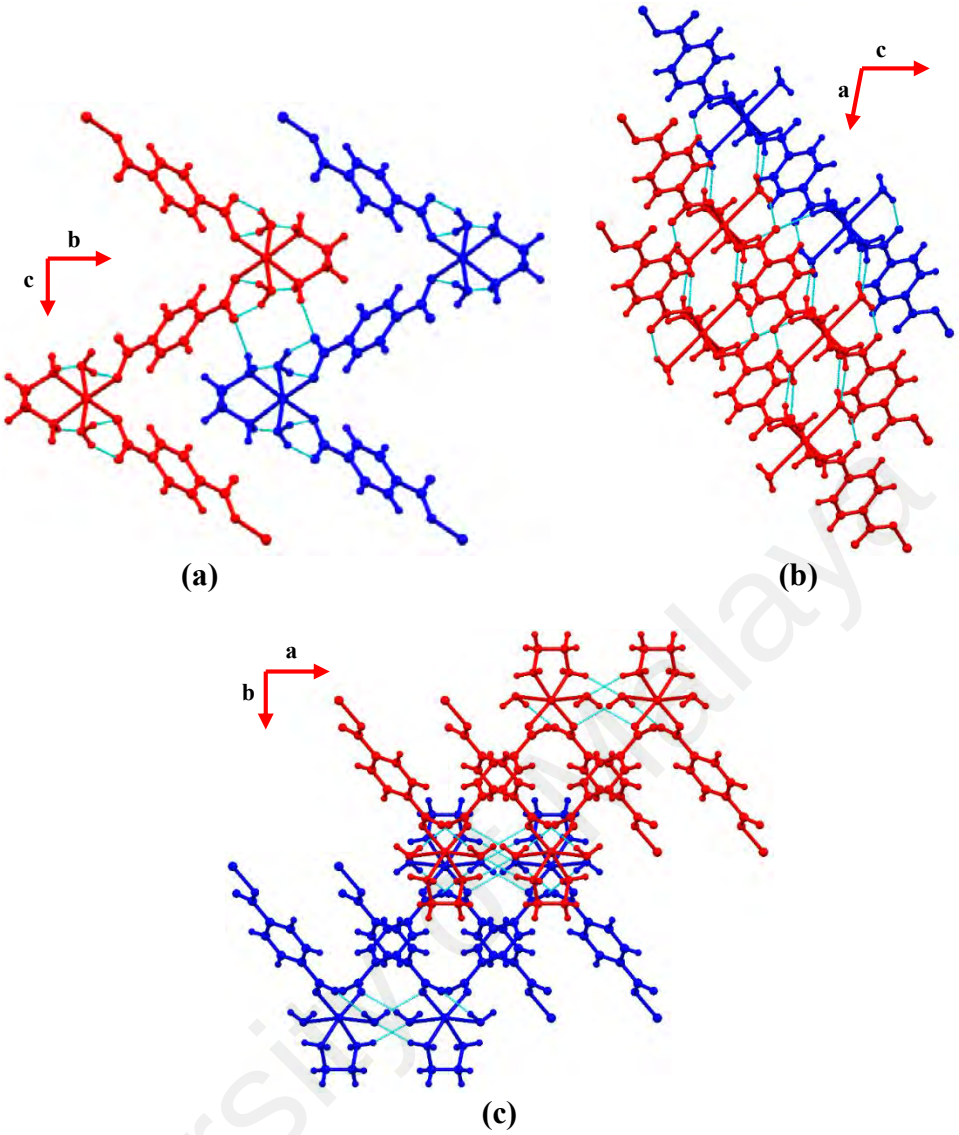

Figure 3.13: Crystal packing of 2; (a), (b) and (c): views along *a*, *b* and *c* axes.

The repeated motifs lead to a 3-dimensional layer as shown in **Figure 3.13**. The hydrogen bonds are depicted in cyan blue. Blue and red indicate different layers of the polymeric zigzag chain.

3.2.3 Crystal 3 $[Ni(en)(L1)(H_2O)_2]\cdot H_2O$

Single crystal X-ray diffraction analysis reveals that **3** crystallized in the triclinic crystal system with $\boldsymbol{P\bar{1}}$ space group. The asymmetric unit contains one L1 linker, one ethylenediamine ligand, two water molecules coordinated to nickel metal ion and one solvated water molecule as shown in **Figure 3.14**. The molecular structure is shown in **Figure 3.15** due to the existence of the inversion centre in the structure.

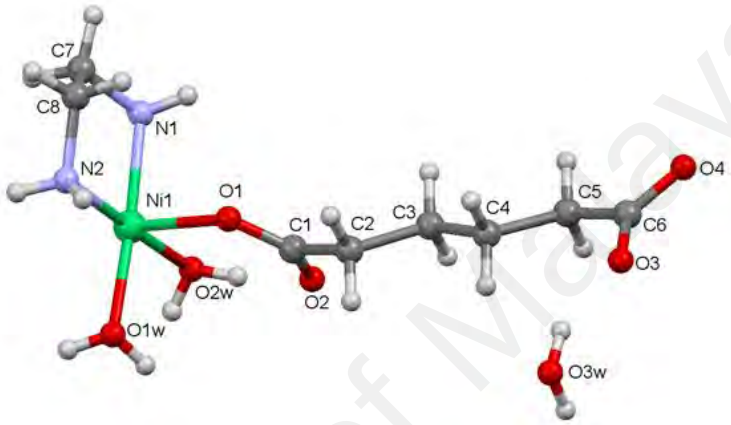

Figure 3.14: Asymmetric unit of 3.

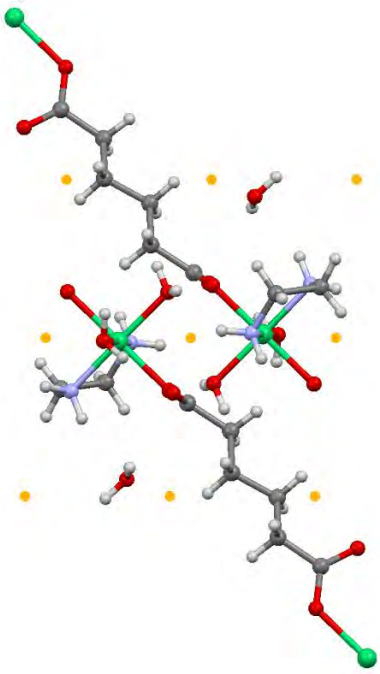

Figure 3.15: View of the centre of inversion in 3 that generates the other part of the structure.

The metal environment can be described as slightly distorted octahedral in which the equatorial positions are occupied by two ethylenediamine nitrogen (Ni1–N1= 2.077(5) Å and Ni1–N2=2.081(5) Å) donors and oxygen from two water molecules O1w and O2w (Ni1–O1w=2.062(5) Å and Ni1–O2w=2.088(4) Å), while the axial position were occupied by deprotonated oxygen atoms O1 and O4 from different bridging L1 linkers. The distortions from the octahedral geometry were indicated by the equatorial position angle of the amine group and water molecule; (N2–Ni1–N1=83.7(2)°, N1–Ni1–O2w=93.92(19)°, N2–Ni1–O1w=89.94(19)° and O1w–Ni1–O2w=92.46(18)°). The four equatorial donors were coplanar (0.019 Å), with the metal atom slightly displaced by 0.062 Å from their mean plane as shown in **Figure 3.16**.

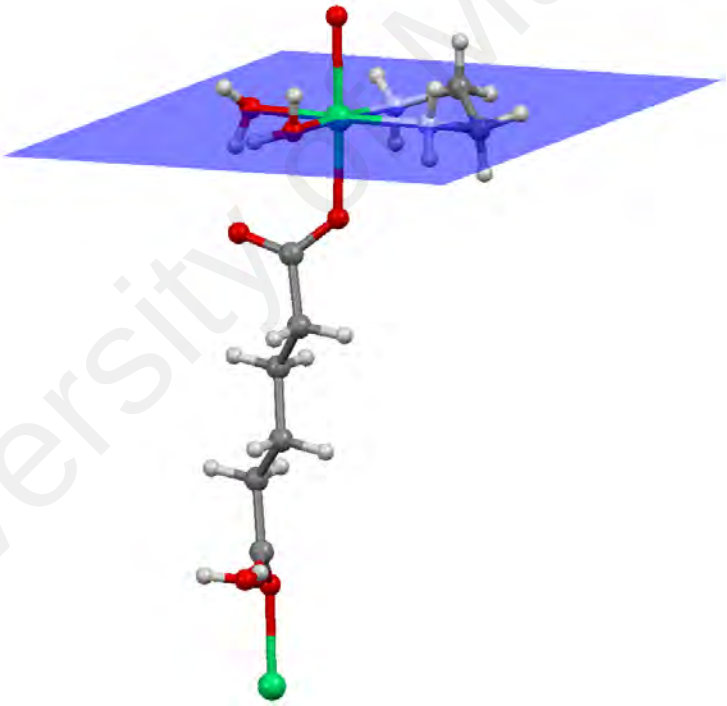

Figure 3.16: Equatorial donor atoms environment, which indicates planarity in 3.

Table 3.4: Hydrogen bonds in 3.

Compound 3				
D ─ H···A	**D ─ H, Å**	**H···A, Å**	**D···A, Å**	**D ─ H···A, °**
O2w–H2wB···O2	0.85	1.81	2.587(6)	152
O3w–H3wB···O3	0.85	2.02	2.804(10)	154
N1–H1A···O3w	0.89	2.29	3.089(9)	148
N1–H1B···O2w	0.89	2.30	3.035(7)	140
N1–H1B···O4	0.89	2.57	3.273(7)	137
N2–H2B···O1w	0.89	2.26	3.037(7)	145
O1w–H1wB···O3	0.85	1.91	2.680(7)	150
O3w–H3wA···O1	0.85	2.57	3.087(9)	120
O1w–H1wA···O2	0.85	1.83	2.662(7)	164

Table 3.4 presents the hydrogen bond synthons for **3**. From the table, most of the hydrogen bonds are contributed by the coordinated as well as the solvated water molecule present in the structure. The intramolecular O–H···O hydrogen bond synthon between oxygen donor from the coordinated water molecule O2w with oxygen from bridging monodentate L1 linker O2 (O2w–H2wB···O2; O···O distance was 2.587(6) Å, angle=152°) contributed to graph set of $S_1^1[6]$ as depicted in **Figure 3.17**. In the structure, the solvated water molecule moiety participates in making intermolecular hydrogen bond synthon by acting as donor with oxygen from bridging L1 linker O3 (O3w–H3wB···O3; O···O distance was 2.804(10) Å, angle=154°) and acts as acceptor with nitrogen from coordinated ethylenediamine N1 (N1–H1A···O3w; N···O distance was 3.089(9) Å, angle=148°) connecting different polymeric Ni(II) ion moiety as shown in the same figure.

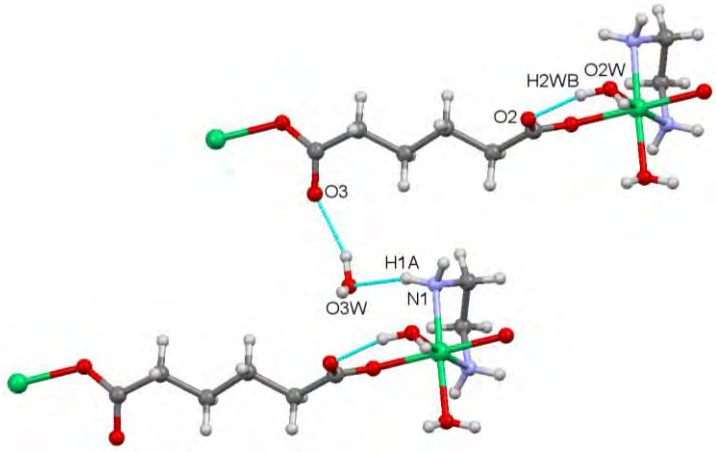

(a)

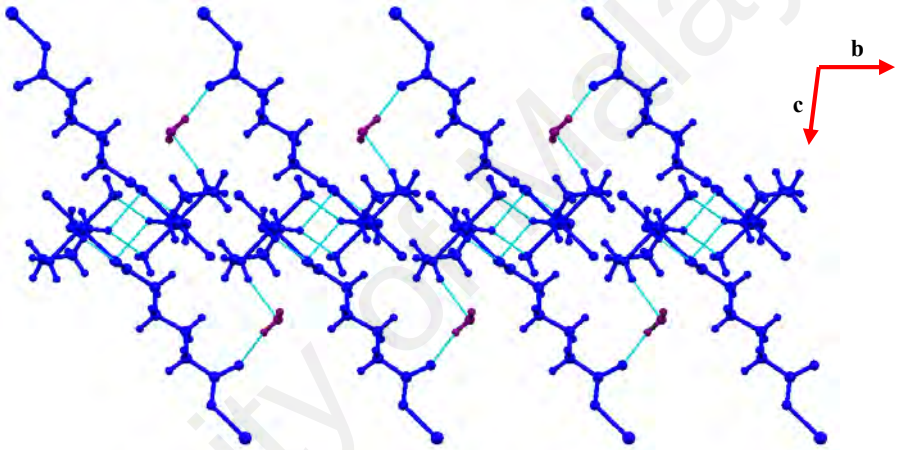

(b)

Figure 3.17: Hydrogen bond synthons from solvated water moiety; (a) connecting different layers, (b) viewed from *a*.

The bifurcated hydrogen bond from the coordinated nitrogen N1 to oxygen atoms from coordinated water molecule O2w and coordinated L1 linker O4 (N1–H1B···O2w; N···O distance was 3.035(7) Å, angle=140°, N1–H1B···O4; N···O distance was 3.273(7) Å, angle=137°) connecting the layer of polymeric chain in **3** contributed to the graph set of $R_2^1[4]$ as shown in **Figure 3.18**.

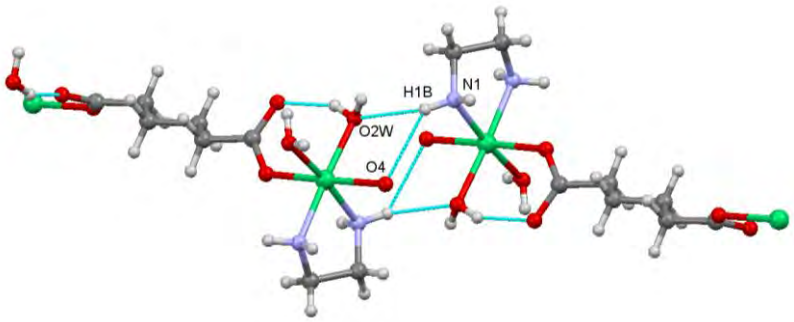

Figure 3.18: The bifurcated hydrogen from nitrogen donor connecting the linear polymeric chain of 3.

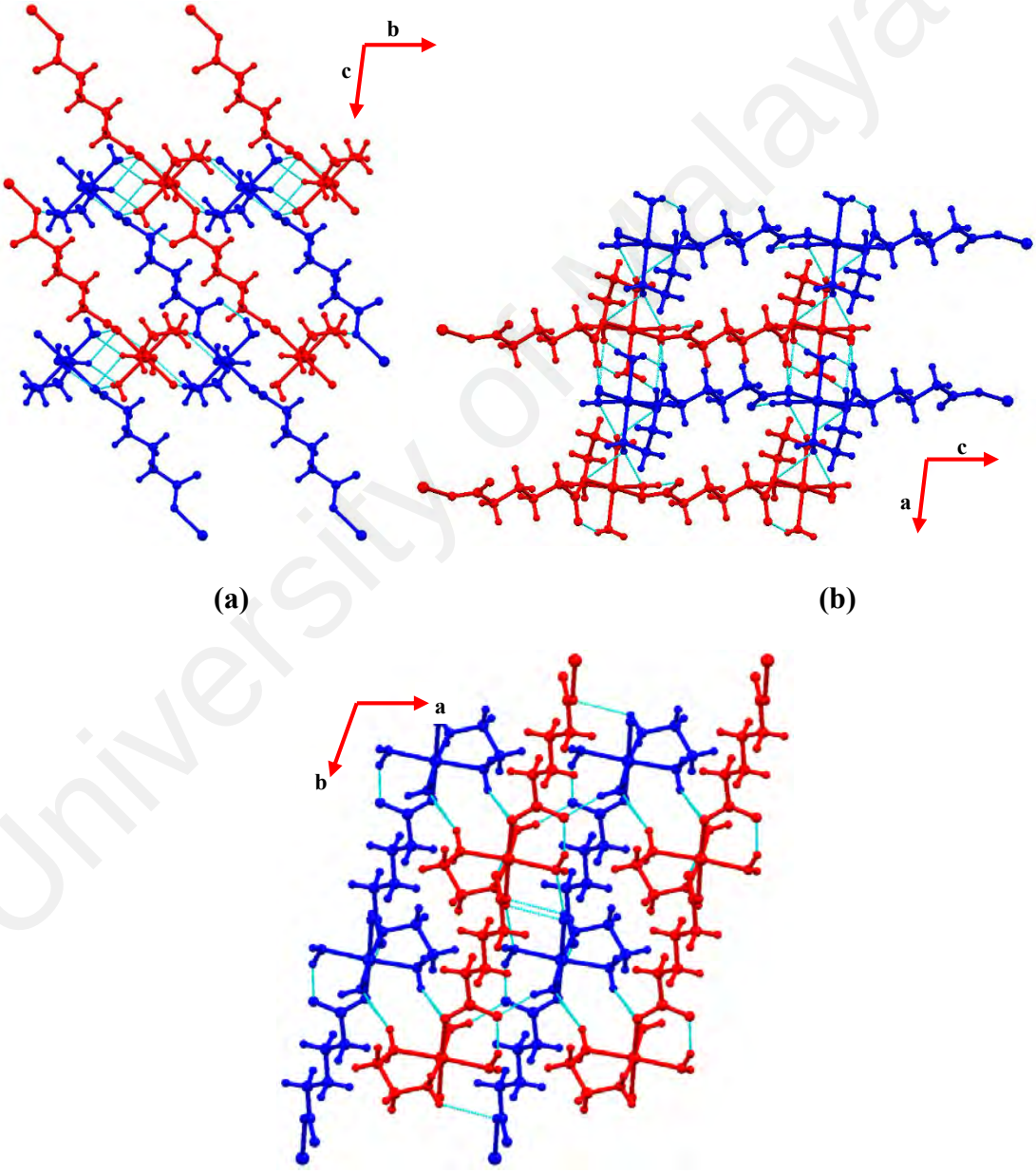

(a) **(b)**

(c)

Figure 3.19: The crystal packing of 3; (a) view from *a*, (b) view from *b* and (c) view from *c* axes.

All the synthons lead to the 2-dimensional linear chains of the crystal packing of **3** as shown in **Figure 3.19**. The hydrogen bonds are depicted in cyan blue. Blue and red indicate different layers of polymeric chains.

3.2.4 Crystal 4 [Ni(o-phen)$_2$(L2)]

Single crystal X-ray diffraction analysis revealed that **4** crystallized in the triclinic crystal system with $P\bar{1}$ space group. The asymmetric unit contained half of L2 linker, and one o-phenylenediamine ligand was coordinated to copper metal ion as shown in **Figure 3.20**. The molecular structure (**Figure 3.21)** was generated by the existence of the centre of inversion (three different centres of inversion). Yellow dots indicate the centre of inversion in the crystal packing. This leads to 1-dimensional linear chains viewed along *a* axis (**Figure 3.22**).

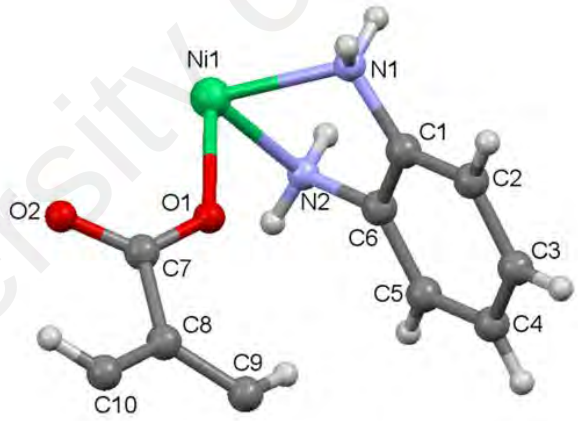

Figure 3.20: **Asymmetric unit of crystal 4**

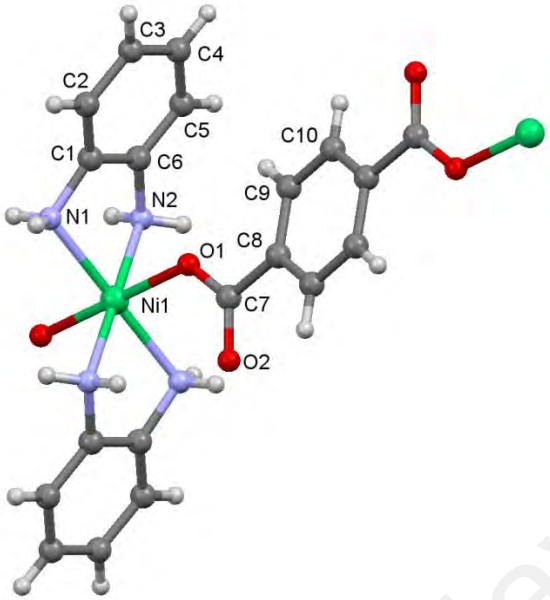

Figure 3.21: Molecular structure of crystal 4

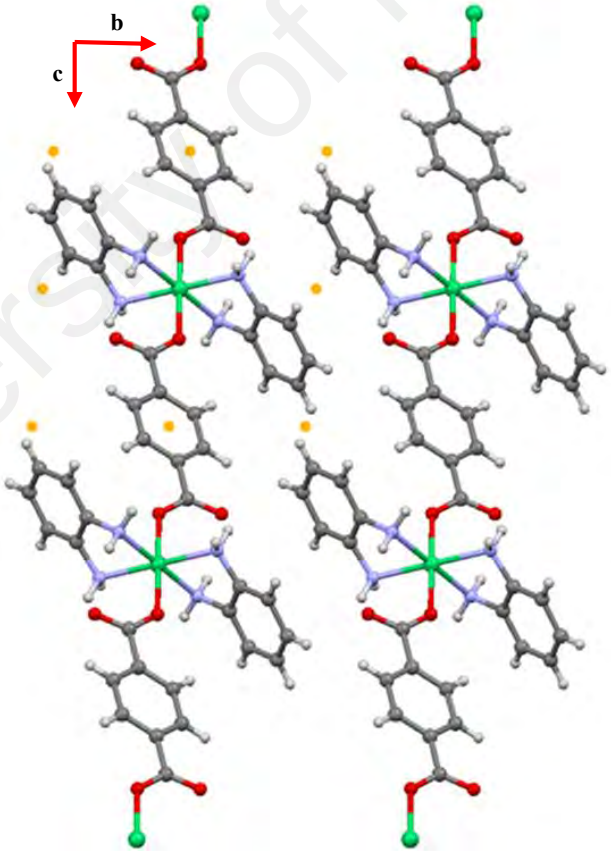

Figure 3.22: 1-dimensional linear polymeric chain of 4 viewed along *a*.

The Ni(II) complex adopts a slightly distorted octahedral geometry, coordinated by four N (Ni1–N1=2.149(14) Å and Ni1–N2=2.137(14) Å) atom from two o-phenylenediamine ligand in the equatorial position and the axial position were occupied by the deprotonated oxygen atoms O1 from different monodentate bridging L2 linker. The distortions from the octahedral geometry are indicated by the equatorial position angle of both amine group and deprotonated oxygen of L2 linker; (N2–Ni1–N1=75.99(5)°, N2–Ni1–N1'=104.01(5)°, N1–Ni1–N2'=104.01(5)° and N1'–Ni1–N2'=75.99(5)°. The four equatorial donors were perfect co-planar, which lay perfectly on the same plane (**Figure 3.23).** The aromatic ring of the L2 linker and o-phenylenediamine in the structure did not contribute to any π-π interaction in the crystal packing because the distance between the rings was 5.436 Å respectively which exceeded the distance for normal π-π interactions.

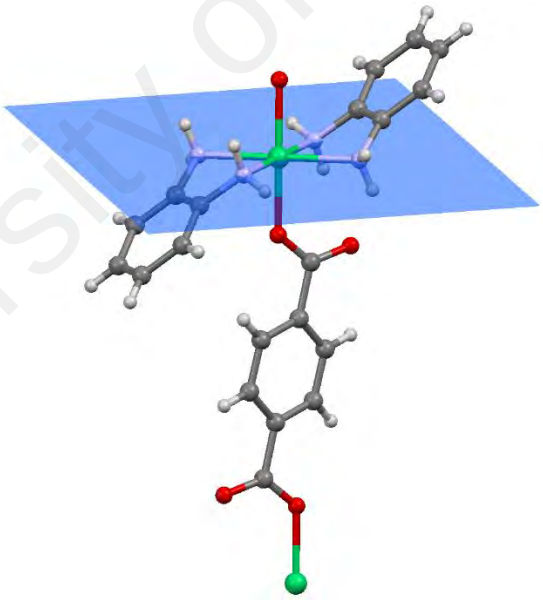

Figure 3.23: The equatorial donor atoms environment, which indicates planarity in 4.

Table 3.5: Hydrogen bonds in 4.

Compound 4				
D ─ H···A	**D ─ H, Å**	**H···A, Å**	**D···A, Å**	**D ─ H···A, °**
N1–H1B···O2	0.89	2.10	2.9749(16)	167
N1–H1A···O2	0. 89	2.32	2.9850(16)	131
N2–H2B···O2	0. 89	2.26	2.9408(18)	133

Table 3.5 presents the hydrogen bond synthons for **4.** From the table, three hydrogen synthons can be observed in the crystal packing. One N–H···O intermolecular hydrogen bond synthons between the nitrogen from o-phenylenediamine N1 with uncoordinated oxygen of monodentate L2 linker O2(N1–H1B···O2, N···O distance was 2.9749(16) Å, angle=167°) were observed between the 1-dimensional polymeric chain of structure **4** which contributed to $C_1^1[3]$ graph set (**Figure 3.24)**.

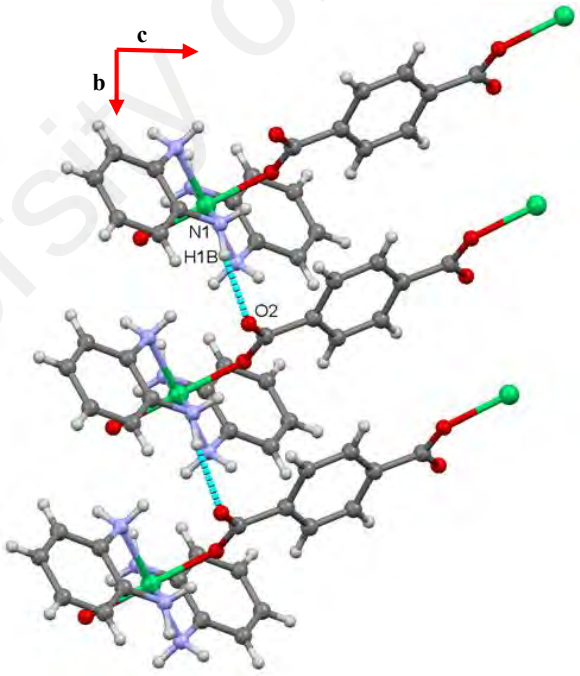

Figure 3.24: Intermolecular N–H···O hydrogen bond synthons environment viewed along *b*.

Two intramolecular N–H···O hydrogen bond synthons were observed as shown in **Figure 3.25** between the nitrogen atom from o-phenylenediamine as donor with uncoordinated oxygen of monodentate L2 linker O2(N1–H1A···O2; N···O distance was 2.9850(16) Å, angle=131° and N2–H2B···O2, N···O distance was 2.9408(18) Å, angle=133°) showing 1-dimensional chains, represented by graph set $S^{1}_{1}[6]$.

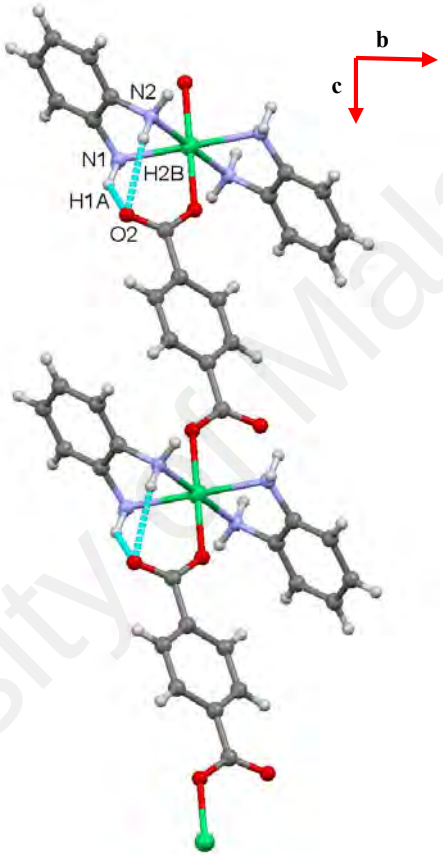

Figure 3.25: Intramolecular hydrogen bond synthons environment around 4 viewed along *a*.

Overall, the synthons also lead to 3-dimensional layers as shown in **Figure 3.26.** The hydrogen bond is depicted in cyan blue. Blue and red indicate different layers of polymeric linear chain.

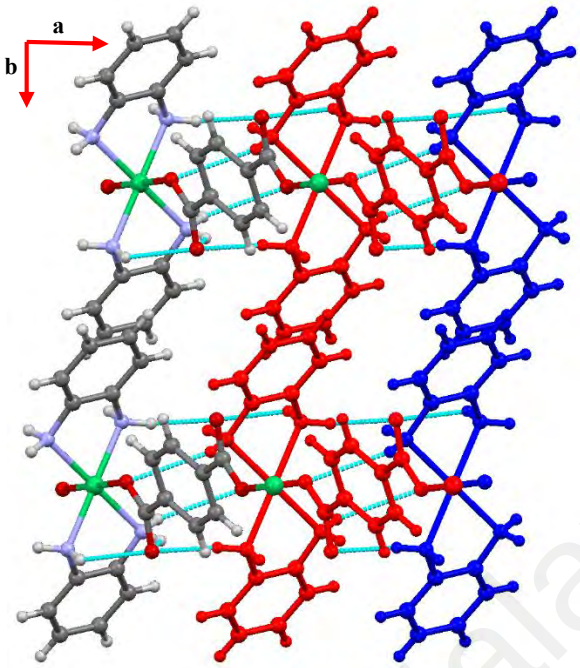

Figure 3.26: 3-dimensional layers of 4 viewed along *c*.

3.2.5 Crystal 5 [$Ni_2(en)_2(L2)_2(H_2O)$]

Single crystal X-ray diffraction analysis revealed that **5** crystallized in the orthorhombic crystal system with *Fddd* space group. The asymmetric unit contained two of half L2 linker, one ethylenediamine ligand, and one water molecules coordinated to nickel metal ion **Figure 3.27**. The molecular structures shown in **Figure 3.28** are generated by the symmetry element existed in the crystal packing.

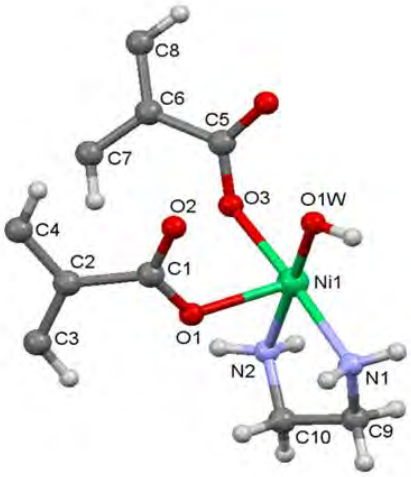

Figure 3.27: **Asymmetric unit of crystal 5.**

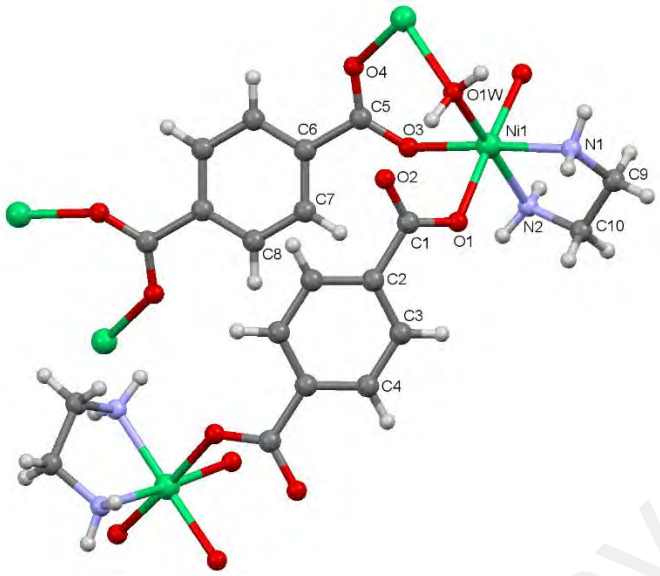

Figure 3.28: Molecular structure of 5.

The metal environment can be described as slightly distorted octahedral in which the equatorial positions are occupied by both the ethylenediamine nitrogen (Ni1–N1= 2.082(19) Å and Ni1–N2=2.083(2) Å) donors, oxygen from one water molecule O1w (Ni1–O1w= 2.0694(12) Å) and bidentate L2 linker O3(Ni1–O3= 2.0453(15) Å), in which another oxygen O4 was coordinated to another nickel metal centre, O4(Ni1–O4= 2.0573(16)Å) in the axial position. The L2 linker and water molecules became the bridging ligand and linker to another nickel metal centre. The other axial position was occupied by the deprotonated oxygen atoms O1(Ni1–O1= 2.0573(16)Å) different bridging L2 linkers. The distortions from the octahedral geometry were indicated by the equatorial position angle of the amine group, water molecule and monodentate L2 linker; (N2–Ni1–N1= 83.65(9)°, N2–Ni1–O3= 93.30(8)°, O3–Ni1–O1w= 91.09(6)° and O1w–Ni1–N1= 91.73(7)°). The four equatorial donors were coplanar (0.035 Å), with the metal atom slightly displaced by 0.060 Å from their mean plane as shown in **Figure 3.29**.

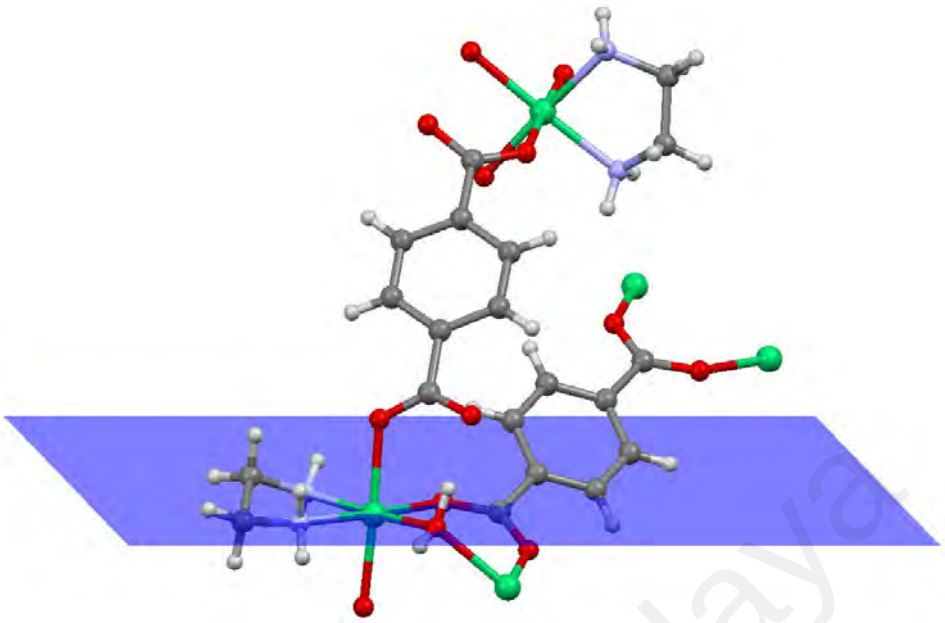

Figure 3.29: The equatorial donor atoms environment, which indicates planarity in 5.

Table 3.6: Hydrogen bonds in 5.

Compound 5				
D ─ H···A	**D ─ H, Å**	**H···A, Å**	**D···A, Å**	**D ─ H···A, °**
O1w–H1w···O2	0.89	1.71	2.5664(18)	163
N1–H1B···O2	0.89	2.12	2.9850(3)	164
N2–H2B···O3	0.89	2.24	3.0250(3)	147

Table 3.6 presents the hydrogen bond synthons for **5.** One intramolecular O–H···O hydrogen bond synthon between oxygen donor from coordinated water molecule O1w with oxygen from uncoordinated L2 linker O2 (O1w–H1w···O2; O···O distance was 2.566(18) Å, angle=163°) contributed to graph set of $S\begin{matrix}1\\1\end{matrix}[6]$ as shown in **Figure 3.30.**

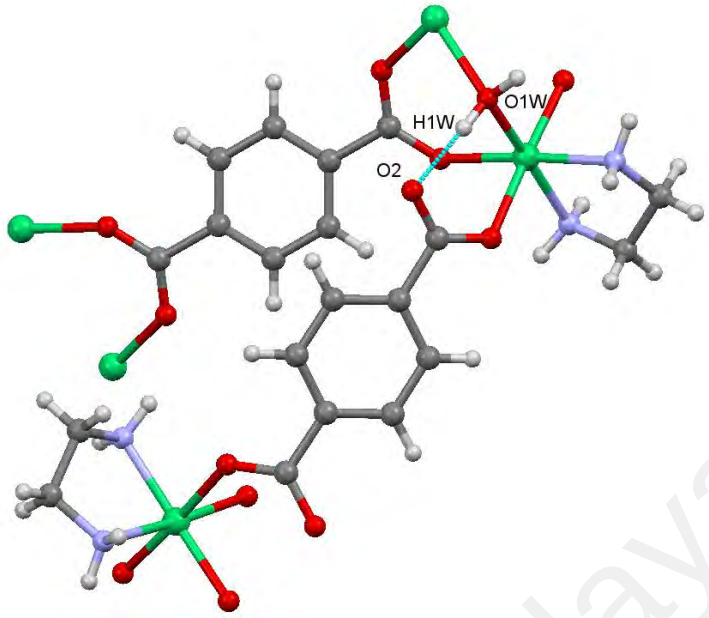

Figure 3.30: Intramolecular hydrogen bond synthons environment in 5.

Nitrogen atoms N1 and N2 from coordinated ethylenediamine participated in making intermolecular N–H···O hydrogen bond synthons with uncoordinated oxygen from L2 linker O2 (N1–H1B···O2; N···O distance are 2.9850(3) Å, angle=164°) and oxygen from monodentate L2 bridging linker O3(N2–H2B···O3; N···O distance was 3.0250(3)) Å, angle=147°) were observed in the structure. N1–H1B···O2 and O1w–H1w···O2 contributed to graph set of $R_2^1[6]$ as shown in **Figure 3.31.**

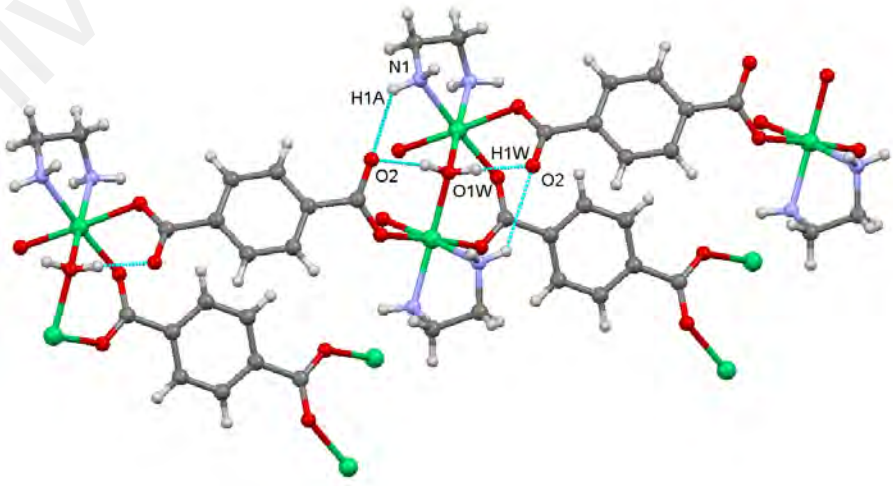

Figure 3.31: Hydrogen bond synthon in 5.

The 3-dimensional polymeric chain leading to a porous network of supramolecular structure of **5** is shown in **Figure 3.32**. Hydrogen bonds are depicted in cyan blue. Blue and red indicate different layers in the crystal packing.

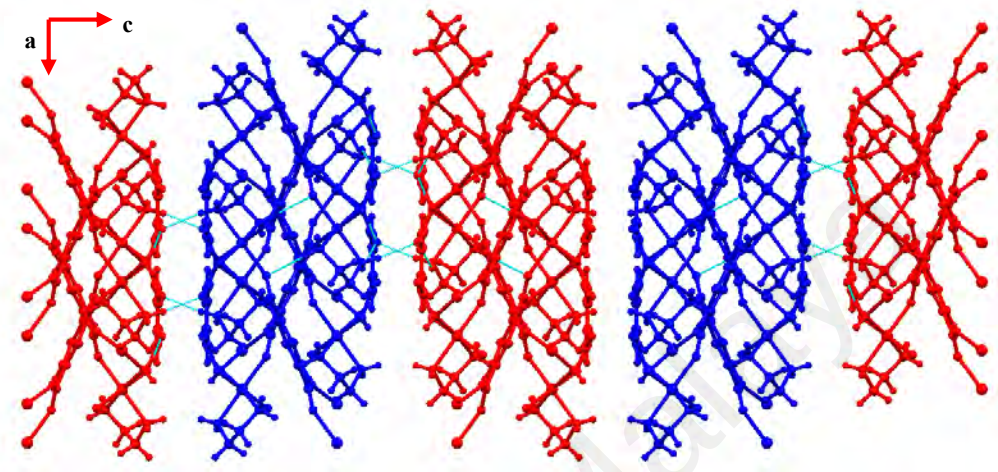

Figure 3.32: Crystal packing of 5 view along *b*-axes.

3.2.6 Crystal 6 [Cd(en)(L2)(H_2O)]

Single crystal X-ray diffraction analysis reveals that **6** crystallized in the monoclinic crystal system with *P* $2_1/c$ space group. The asymmetric unit contained one Cd(II) ion, one terepthalic ligand, one ethylenediamine ligand, and one water molecule coordinated to the cadmium metal centre as shown in **Figure 3.33**. The molecular structure shown in **Figure 3.34** was generated by the existence of 2-fold rotation symmetry and inversion centre in the packing as depicted in **Figure 3.35.**

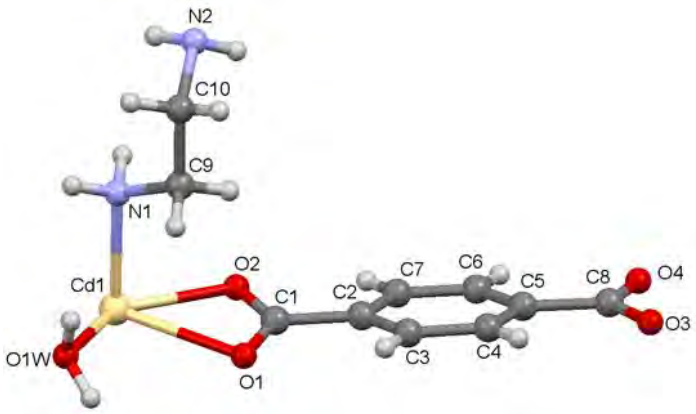

Figure 3.33: Asymmetric unit of crystal 6

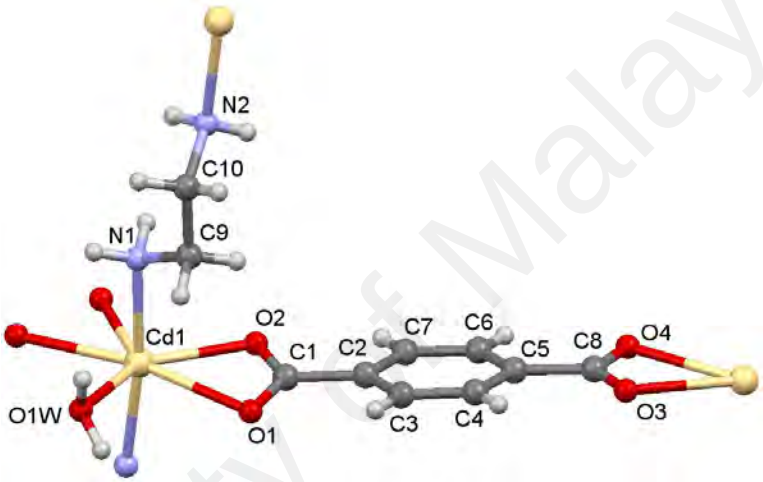

Figure 3.34: Molecular structure of 6

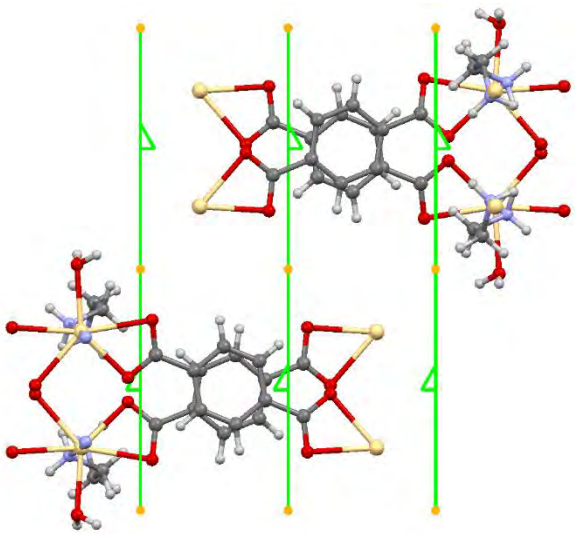

Figure 3.35: View of 2-fold symmetry rotation axis and centre of inversion in 6 that generates the other part of the structure in the crystal packing.

The Cd(II) ion complex adopted a slightly distorted pentagonal bipyramidal geometry, coordinated by two nitrogen atom (Cd1–N1=2.279(3) Å and Cd1–N2=2.271(2) Å) atom from two ethylenediamine ligand in axial position, whereas the equatorial position was occupied by four oxygen atoms from different bidentate bridging L2 linker and one oxygen from water. The distortions from the pentagonal bipyramidal geometry were indicated by the equatorial position angle of the oxygen of L2 linker and water coordinated to the Cd metal; (O1–Cd1–O2=53.90(7)°, O2–Cd1–O3=86.79(7)°, O3–Cd1–O4=53.08(7), O4–Cd1–O1w=82.62(8)° and O1w–Cd1–O1= 84.05(7)°). The five equatorial donors were coplanar (0.087 Å), with the metal atom slightly displaced by 0.109 Å from their mean plane as shown in **Figure 3.36.**

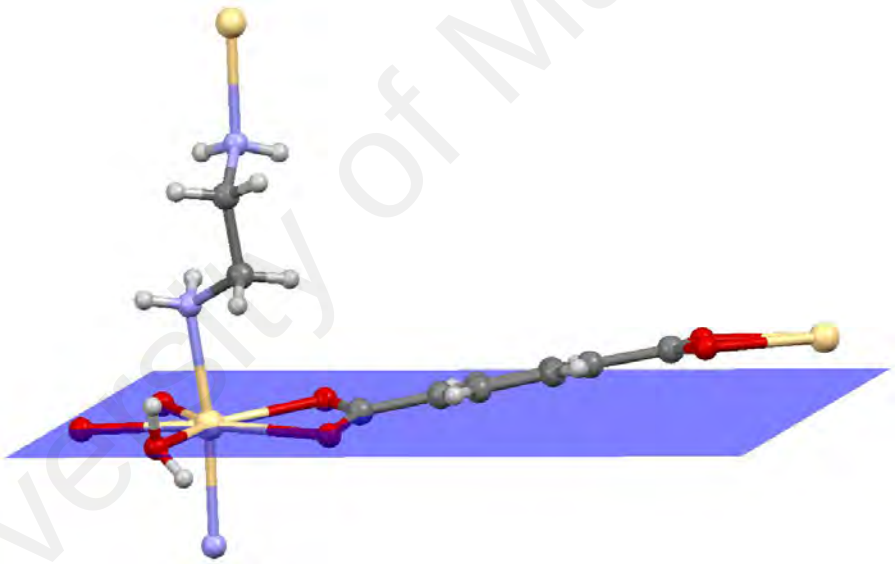

Figure 3.36: The equatorial oxygen atoms environment, which indicates planarity in 6.

Table 3.7: Hydrogen bonds in 6.

Compound 6				
D ─ H···A	**D ─ H, Å**	**H···A, Å**	**D···A, Å**	**D ─ H···A, °**
N2–H2B···O2	0. 89	2.08	2.920(3)	158
N2–H2A···O3	0. 89	2.32	3.095(3)	145
N1–H1A···O3	0.89	2.22	3.091(4)	167
O1w–H1wB···O1	0. 89	1.87	2.723(3)	160

Table 3.7 presents the hydrogen bond synthons for **6.** From the table, four intermolecular hydrogen bond synthons were observed. Nitrogen atom from coordinated ethylenediamine N2 acted as donor thus making two hydrogen bonds with the coordinated L2 linker oxygen O2 and O3 (N2–H2B···O2; N···O distance was 2.920(3) Å), angle=158° and N2–H2A···O3; N···O distance was 3.095(3) Å, angle=145°**)** contributed to the graph set of $R_1^2[6]$ together as shown in **Figure 3.37.** Another nitrogen atom donor from the coordinated ethylenediamnine N1 made the hydrogen bond with one oxygen from coordinated L2 linker O3 (N1–H1A···O3; N···O distance was 3.091(4) Å, angle=167°) which contributed to another set of $R_2^1[7]$ graph set with N2–H2A···O3 synthon as shown in the same figure.

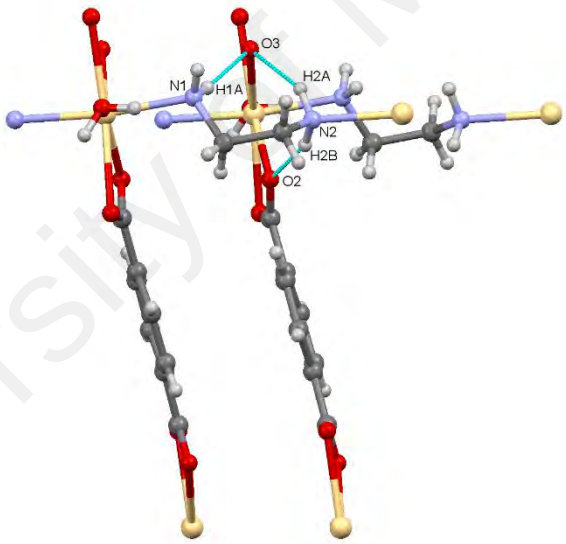

Figure 3.37: N–H···O hydrogen bond synthons in 6.

Oxygen from the coordinated water molecule O1w acted as donor thus making the O–H···O intermolecular hydrogen bond with the coordinated oxygen of L2 linker O1 (O1w–H1wB···O1; O···O distance was 2.723(3) Å, angle=160°) represented by the $C_1^1[3]$ graph set connecting the polymeric layer side by side (**Figure 3.38**).

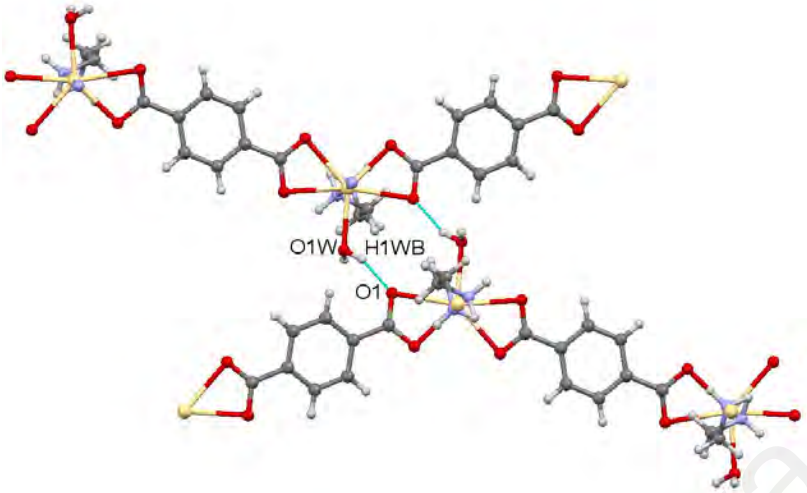

Figure 3.38: O–H···O intermolecular hydrogen bond in 6.

All the synthons leading to the 2-dimensional polymeric interlayer zigzag network of the crystal packing were viewed along the *b* axis as depicted in **Figure 3.39**. Hydrogen bonds are depicted in cyan blue. Different colours indicate different layers of polymeric chain.

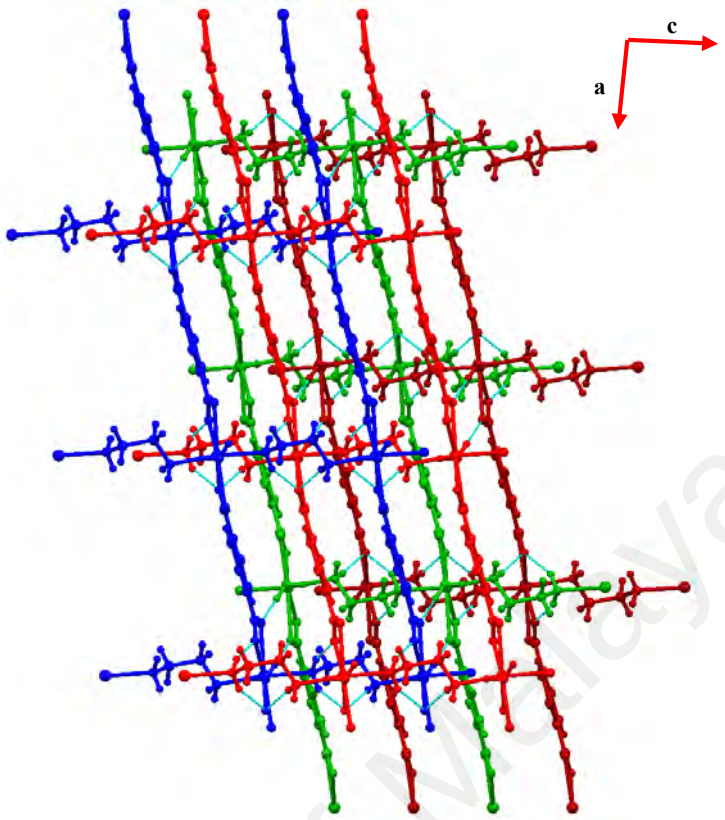

(a)

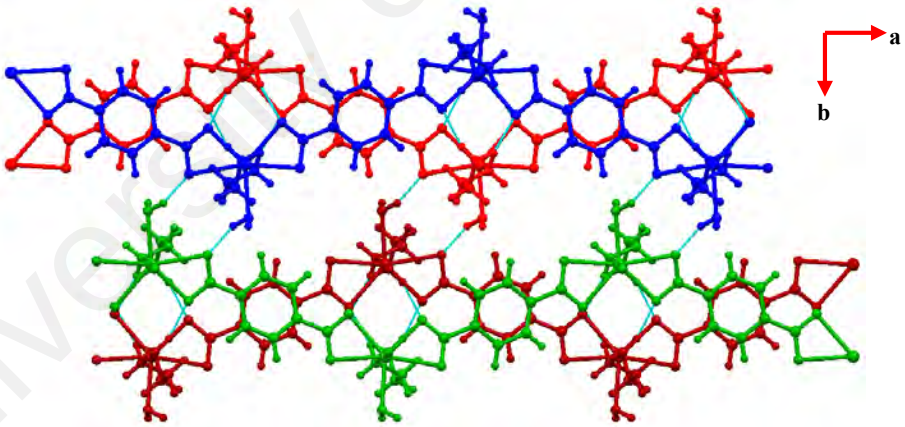

(b)

Figure 3.39: Crystal packing of 6; (a) viewed along *b*, (b) viewed along *c* axes.

Figure 3.40 shows the π-π interaction between the terephthalate rings in **6**. The centroid distance of the slipped π-stacking of the ring was 3.747 Å which is in the range as reported by Janiak (Janiak, 2000).

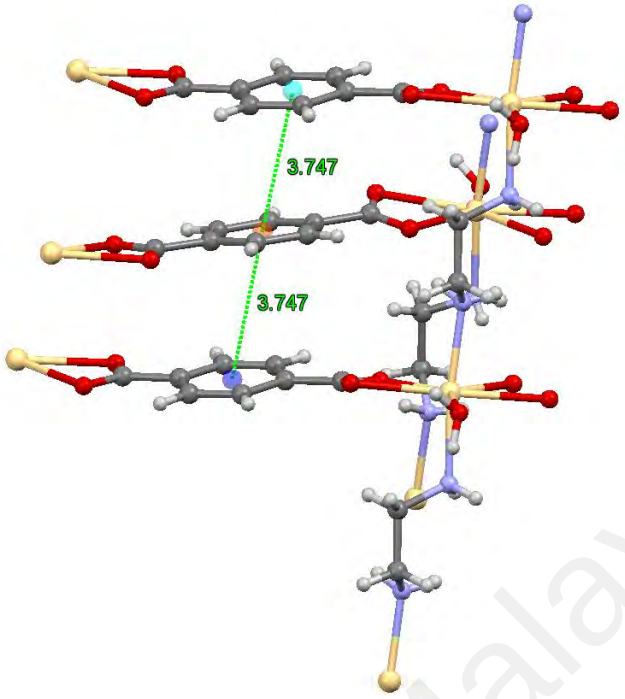

Figure 3.40: **Interlayered chain along *a*-axis showing π-π interactions between the terephthalate rings.**

3.2.7 Crystal 7 [Cd_2(o-phen)$_2$(L1)(Cl)$_2$(H_2O)$_2$]

Single crystal X-ray diffraction analysis revealed that **7** crystallized in the monoclinic crystal system with *P* $2_1/c$ space group. The asymmetric unit contained one Cd(II) ion, half of one L1 linker, one o-phen ligand, one water molecule and one chlorine atom coordinated to cadmium metal centre as shown in **Figure 3.41.** The molecular structure shown in **Figure 3.42** was generated by the 2-fold rotation symmetry and existence of the centre of inversion.

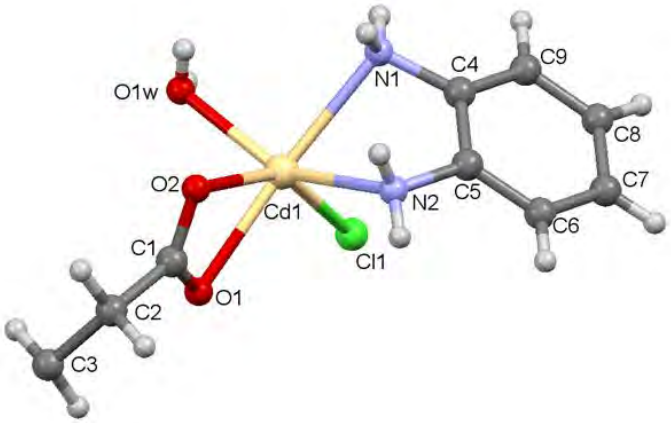

Figure 3.41: Asymmetric unit of 7.

In the structure, the 2-fold rotation symmetry and centre of inversion passed through the middle of C3–C3 bond in the L1 linker. Green line and yellow dots indicate the 2-fold rotation symmetry and centre of inversion, respectively.

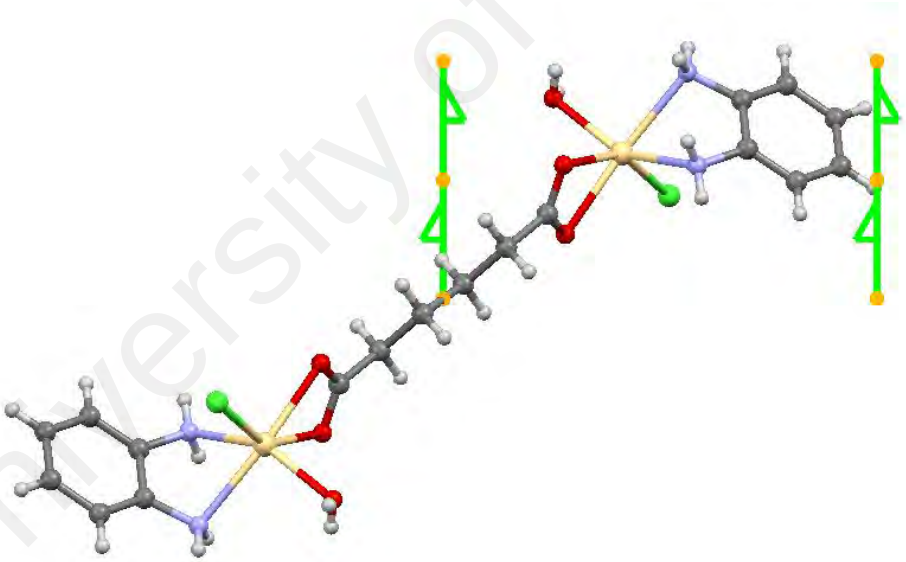

Figure 3.42: View of 2-fold rotation axis and inversion centre in 7 that generates the other part of the structure.

The metal environment of Cd(II)ion that can be described as distorted octahedral in which the axial positions were occupied by one ethylenediamine nitrogen (Cd1–N2=2.396(2) Å donors and oxygen from the coordinated water molecule O1w (Cd1–O1w=2.225(19) Å), whereas the equatorial position was occupied by one

ethylenediamine nitrogen (Cd1–N1=2.447(2) Å) donors, deprotonated oxygen atoms O1 and O2 (Cd1–O1=2.343(18) Å and Cd1–O2=2.356(17) Å) from the bridging bidentate L1 linkers and chlorine atom. The distortions from the octahedral geometry were indicated by the equatorial position angle of one nitrogen from o-phenylenediamine, oxygen from bidentate L1 linker and chlorine atom; (O2–Cd1–O1=55.63(6)°, O1–Cd1–Cl1=94.66(4)°, Cl1–Cd1–N1= 92.72(6)° and N1–Cd1–O2= 115.35(7)°). The four equatorial donors were coplanar (0.015 Å), with the metal atom slightly displaced by 0.327 Å from their mean plane (**Figure 3.43**).

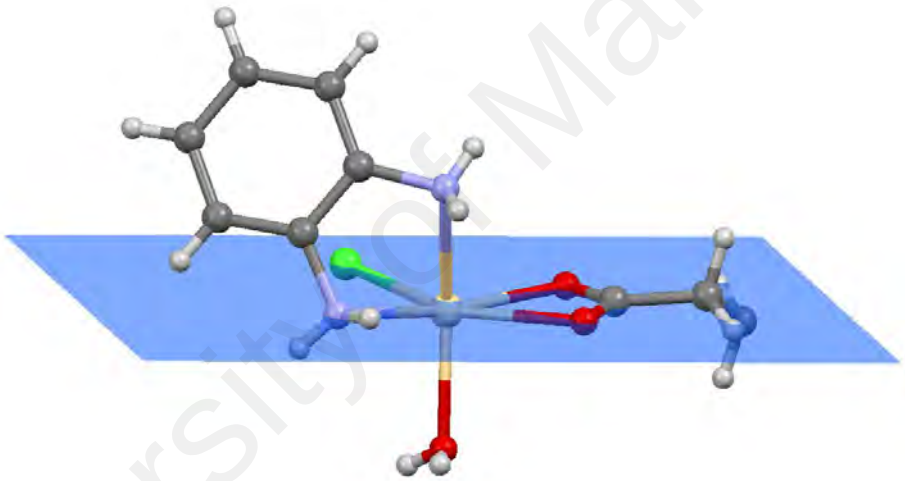

Figure 3.43: The equatorial atoms environment, which indicates planarity in 7.

Table 3.8: Hydrogen bonds in 7.

Compound 7				
D ─ H···A	**D ─ H, Å**	**H···A, Å**	**D···A, Å**	**D ─ H···A, °**
N1–H1A···Cl1	0.82	2.63	3.430(2)	165
N2–H2A···Cl1	0.77	2.63	3.387(3)	168
N1–H1B···Cl1	0.87	2.52	3.374(2)	166
N2–H2B···Cl1	0.82	2.57	3.322(3)	154
O1w–H1wA···O1	0.74	1.99	2.732(3)	176
O1w–H1wB···O2	0.75	1.92	2.670(3)	177

Table 3.8 presents the hydrogen bond synthons of **7**. In the structure, chlorine atom (Cl1) was coordinated to the Cd(II) ion metal centre participated in making weak hydrogen bond as the acceptor with nitrogen atom donor from the coordinated ethylenediamine N1 and N2 (N1–H1A···Cl1; N···Cl distance was 3.430(2)Å, angle=165°, and N2–H2A···Cl1; N···Cl distance was 3.387(3)Å, angle=168°) as shown in **Figure 3.44**. This leads to different layers of the dimeric chain (N1–H1B···Cl1; N···Cl distance was 3.374(2) Å, angle=166°, N···Cl distance was 3.387(3)Å, angle=168°).

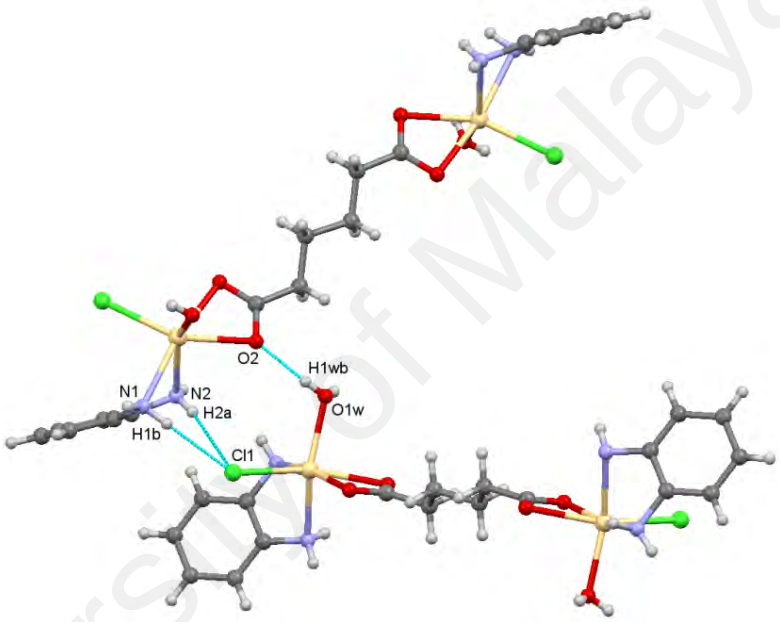

Figure 3.44: Hydrogen bond synthons in 7.

The intermolecular O–H···O hydrogen bond synthon contributed by the coordinated water molecule O1w with oxygen from the bridging bidentate L1 linker O1 and O2 (O1w–H1wA···O1; O···O distance was 2.732(3)Å, angle=168°, and O1w–H1wB···O2; O···O distance was 2.670(3)Å, angle=154°) were shown in the same figure. All the intermolecular hydrogen bond synthons linked the dimeric chain into a one-dimensional structure as shown in **Figure 3.45.** Hydrogen bonds are depicted in cyan blue. Blue and red colours indicate different layers of chain.

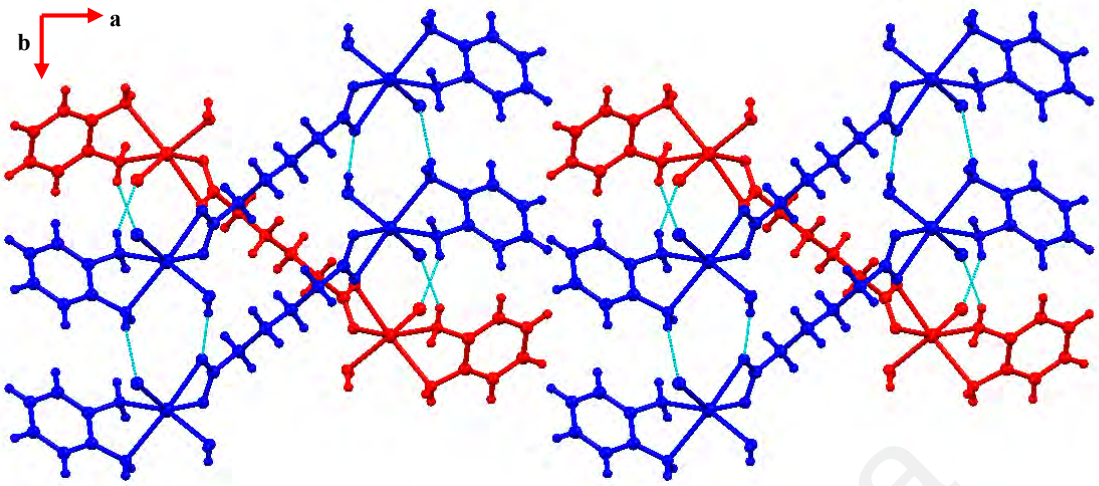

Figure 3.45: Packing of 7 viewed along *c* axes.

Table 3.9: Selected bond lengths (Å) and angles (°) for the metal coordination centers of 1, 2, 3, 4, 5, 6, and 7.

1	
Cu1–O1	1.994(9)
Cu1–O1^{a}	1.994(9)
Cu1–N1^{a}	1.989(11)
Cu1–N1	1.989(11)
O1^{a} –Cu1–O1	89.67(5)
N1^{a} –Cu1–O1^{a}	166.23(4)
N1^{a} –Cu1–O1	93.70(4)
N1^{a} –Cu1–O1	93.70(4)
N1^{a} –Cu1–N1	86.17(6)
Symmetry transformations used to generate equivalent atoms: *(a) 1-X,+Y,1/2-Z*	
2	
Cu1–O2	1.955(2)
Cu1–O2^{b}	1.955(2)
Cu1–N1	2.005(2)
Cu1–N1^{b}	2.005(2)
Cu1–O1w	2.653(3)
O2–Cu1–O2^{b}	90.41(14)
O2–Cu1–N1	93.23(10)
N1^{b} –Cu1–O2^{b}	93.23(10)
N1^{b}–Cu1–N1	84.87(13)
Symmetry transformations used to generate equivalent atoms: *(b) 1-X,+Y,3/2-Z*	
3	
Ni1–O1	2.087(4)
Ni1–O1w	2.062(5)
Ni1–O2w	2.088(4)
Ni1–O4	2.110(4)
Ni1–N1	2.077(5)
Ni1–N2	2.081(5)
O1w–Ni1–O2w	92.46(18)
N1–Ni1–O2w	93.92(19)
N2–Ni1–O1w	89.94(19)
N2–Ni1–N1	83.7(2)
O4–Ni1–O1	178.52(17)

4	
Ni1–O1^{c}	2.063(11)
Ni1–O1	2.063(11)
Ni1–N1	2.149(14)
Ni1–N1^{c}	2.149(14)
Ni1–N2^{c}	2.137(14)
Ni1–N2	2.137(14)
N2–Ni1–N1	75.99(5)
N2–Ni1–N1^{c}	104.01(5)
N2^{c} –Ni1–N1	104.01(5)
N2^{c} –Ni1–N1^{c}	75.99(5)
O1–Ni1–O1^{c}	180.0
Symmetry transformations used to generate equivalent atoms: *(c) -X,1-Y,1-Z*	
5	
Ni1–O1	2.1031(15)
Ni1–O1w	2.0694(12)
Ni1–O3	2.0453(15)
Ni1–O4^{d}	2.0573(16)
Ni1–N1	2.0822(19)
Ni1–N2	2.083(2)
O1w–Ni1–O3	91.09(6)
O3–Ni1–N2	93.30(8)
N1–Ni1–N2	83.65(9)
N1–Ni1–O1w	91.73(7)
O4^{d} –Ni1–O1	176.89(7)
Symmetry transformations used to generate equivalent atoms: *(d) 3/4-X,3/4-Y,+Z*	
6	
Cd1–O1	2.531(2)
Cd1–O1w	2.374(2)
Cd1–O2	2.334(2)
Cd1–O3^{e}	2.479(2)
Cd1–O4^{e}	2.453(2)
Cd1–N1	2.279(3)
Cd1–N2^{f}	2.271(2)
O1w-Cd1-O1	84.05(7)
O1w-Cd1-O4^{e}	82.62(8)
O2-Cd1-O1	53.90(7)

O2-Cd1-O3^{e}	86.79(7)
O4^{e}-Cd1- O3^{e}	53.08(7)
N2^{f}-Cd1-N1	173.07(9)
Symmetry transformations used to generate equivalent atoms*: (e) -1+X,3/2-Y, (f) +X,+Y,-1+Z*	
7	
Cd1–Cl1	2.528(6)
Cd1–O1	2.343(18)
Cd1–O1w	2.225(19)
Cd1–O2	2.356(17)
Cd1–N1	2.447(2)
Cd1–N2	2.396(2)
O1-Cd1-Cl1	94.66(4)
O1-Cd1-O2	55.63(6)
N1-Cd1-Cl1	92.72(6)
N1-Cd1-O2	115.35(7)
N2-Cd1-O1w	149.23(9)

Table 3.10: Crystal data and structure parameters for crystal 1, 2, 3, 4, 5, 6 and 7

Complex	1	2	3	4	5	6	7
Empirical Formula	$C_{14}H_{26}CuN_2O_8$	$C_{10}H_{16}CuN_2O_6$	$C_8H_{22}N_2NiO_7$	$C_{20}H_{20}N_4NiO_4$	$C_{20}H_{26}N_4Ni_2O_9$	$C_{10}H_{14}CdN_2O_5$	$C_{18}H_{28}Cd_2C_{l2}N_4O_6$
CCDC No	1450394	1450395	1450396	1450397	1472497	1450393	1446968
Formula weight	413.92	323.79	316.97	439.10	583.87	354.64	692.17
Crystal System	Monoclinic	Monoclinic	Triclinic	Triclinic	Orthorhombic	Monoclinic	Monoclinic
Space group	*C* 2/c	*P* 2/c	$P\bar{1}$	$P\bar{1}$	*Fddd*	$P\,2_1/c$	$P\,2_1/c$
a(Å)	13.4222(9)	5.7227(2)	8.2248(12)	5.4363(3)	10.6396(6)	10.4872(4)	20.4710(8)
b (Å)	14.3085(10)	8.7895(3)	8.9689(13)	9.2157(5)	21.0757(13)	16.9694(8)	5.5578(2)
c (Å)	9.1153(6)	12.8488(5)	9.4334(10)	9.3172(4)	42.746(3)	7.4680(4)	10.7910(3)
α (°)	90	90	95.58(1)	93.279(4)	90	90	90
ß (°)	94.481(6)	101.072(3)	94.868(10)	97.716(4)	90	98.467(4)	98.122(3)
ɤ (°)	90	90	107.906(13)	97.926(4)	90	90	90
Volume (Å^3)	1745.3(2)	634.26(4)	654.17(16)	456.77(4)	9585.3(10)	1314.54(10)	1215.41(8)
Z	4	2	2	1	16	4	2
$D_{calcd.}$ (g cm^3)	1.5752	1.6953	1.6090	1.5962	1.618	1.7918	1.8912
F(000)	869.8	334.9	336.9	228.4	4832	701.1	681.6
μ (mm^{-1})	1.296	1.747	1.511	1.099	1.629	1.675	2.010
Reflection collected	4968	4457	5714	8352	15659	17197	15862
Independent reflections	2282 [R_{int} = 0.0228]	1319 [R_{int} = 0.0400]	3082 [R_{int} = 0.0656]	2488 [R_{int} = 0.0302]	3304 [R_{int} = 0.0421]	3654 [Rint = 0.0370]	2506 [Rint = 0.0387]
GOF on F²	1.029	1.047	1.036	1.037	1.054	1.057	1.070
Final R indices [I >2σ(I)]	R_1=0.0239, wR_{2_2}=0.0603	R1=0.0356, wR_2=0.0821	R1=0.0774, wR_2=0.2335	R1=0.0305, wR_2=0.0723	R_1 = 0.0377, wR_2 = 0.0725	R1=0.0324, wR_2=0.0767	R1=0.0227, wR_2=0.0516
Final R indices (all data)	R1=0.0259, wR_2=0.0618	R1=0.0434, wR_2=0.0866	R1=0.1007, wR_2=0.2626	R1=0.0334, wR_2=0.0751	R1=0.0545, wR_2=0.0807	R1=0.0376, wR_2=0.0813	R1=0.0268, wR_2=0.0540

3.3 Powder X-ray Diffraction Analysis

The PXRD experiment was conducted to confirm the structural homogeneity of the bulk material sample. This was done by comparing the precipitates reduced from the solution with the simulated powder x-ray pattern. The observed PXRD pattern for the bulk material of complexes **1**, **2**, **3**, **4**, **5**, **6,** and **7** were found to be consistent with the calculated pattern generated using the single crystal X-ray diffraction, indicating the purity of the bulk material. The agreement indices in the form of R profile after the fitting mode refinement with the calculated powder pattern from crystallographic information file (CIF) of the crystal structure were found to be coherent from the general accepted R profile <30%.

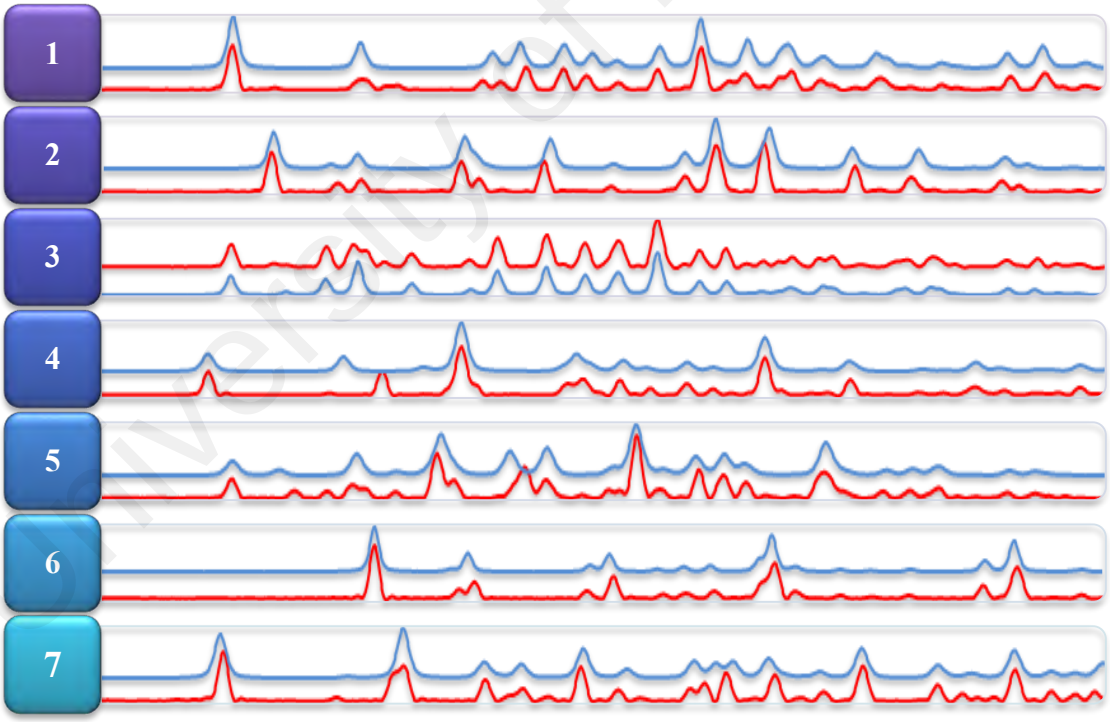

Figure 3.46: PXRD spectrums of bulk powder of single crystal of 1, 2, 3, 4, 5, 6 and 7. Red line represents the bulk products whereas blue line represents PXRD diffraction patterns simulated from the single crystal structures.

3.4 Application on dye adsorption studies: Solid Phase Adsorption (SPA)

3.4.1 Optimization of parameters affecting the SPA procedures

The sample screening was done for all compounds to calculate the percentage removal of Chicago Sky Blue (CSB) dye as shown in **Figure 3.47** below.

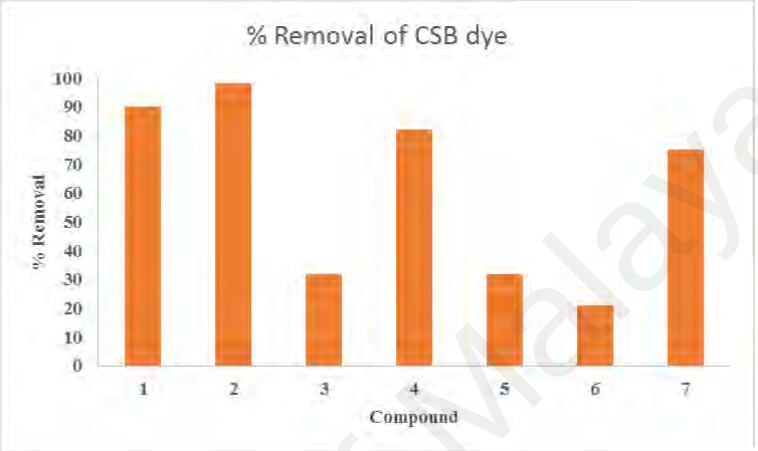

Figure 3.47: Sample screening; 10mg of the crystal in 10ml of CSB for removal experiment.

As shown in the graph, compounds **1**, **2**, **4**, and **7** showed high percentage of the dye removal, which is more than 80%. This indicates that all these four samples have the potential as a dye removal agent. Eventhough the other three crystals showed better percentage of removal, somehow the physical appearance of the crystal had changed. Therefore, these crystals were ineligible to become a dye removal agent. Crystal **7** was chosen for further experiment due to high potential of CSB removal. Further studies highlighting on other factors; pH, adsorbent dosage, time and adsorbent capacity should be conducted to support the results.

3.4.1.1 Effect of the (2) doses on CSB

The mass of **7** was studied within the range of 5 to 30 mg. The results in **Figure 3.48(A)** show that the removal of CSB increased with the increasing dosage of **7**. The quantitative removal of the CSB was obtained using 10 mg of **7;** above 20 mg of adsorbent dosage, the CSB removal remained nearly constant. Therefore, 10 mg of **7** was used for all experiments.

3.4.1.2 Effect of solution pH on the removal of CSB

The effect of solution pH on the removal of CSB dye using **7** was examined at different pH's (i.e., 4.5 - 10.5). As shown in **Figure 3.48(B)**, the graph shows that there are not much changed in the removal percentage of the dye at different pH. The removal percentage of CSB dye (78%) for **7** was achieved at pH 7.5 which was selected for further analysis**.**

3.4.1.3 Effect of contact time on the removal of CSB

The effect of contact time for the removal of CSB dye was studied using **7** at different adsorption times (5 to 40 min) as shown in **Figure 3.48(C)**. The adsorption capacity shows minimal increase for the removal of CSB throughout the period of 40 min. Therefore, 15 min was selected for further experiments.

3.4.1.4 Effect of CSB dye concentration

The effect of initial CSB concentration on the adsorption capacity of **7** was investigated under equilibrium condition at room temperature. The adsorption capacity for 30 mg of **7** with 10 mL of CSB solution (20 - 100 mg L^{-1}) under optimum conditions is shown in **Figure 3.48(D)**. Equation (4) was used to calculate the adsorption capacity of **7** towards CSB dye. From the plot of q_e and C_e, the graph showed that the adsorption

capacity increased with the increasing of CSB concentration until the adsorbent site became saturated.

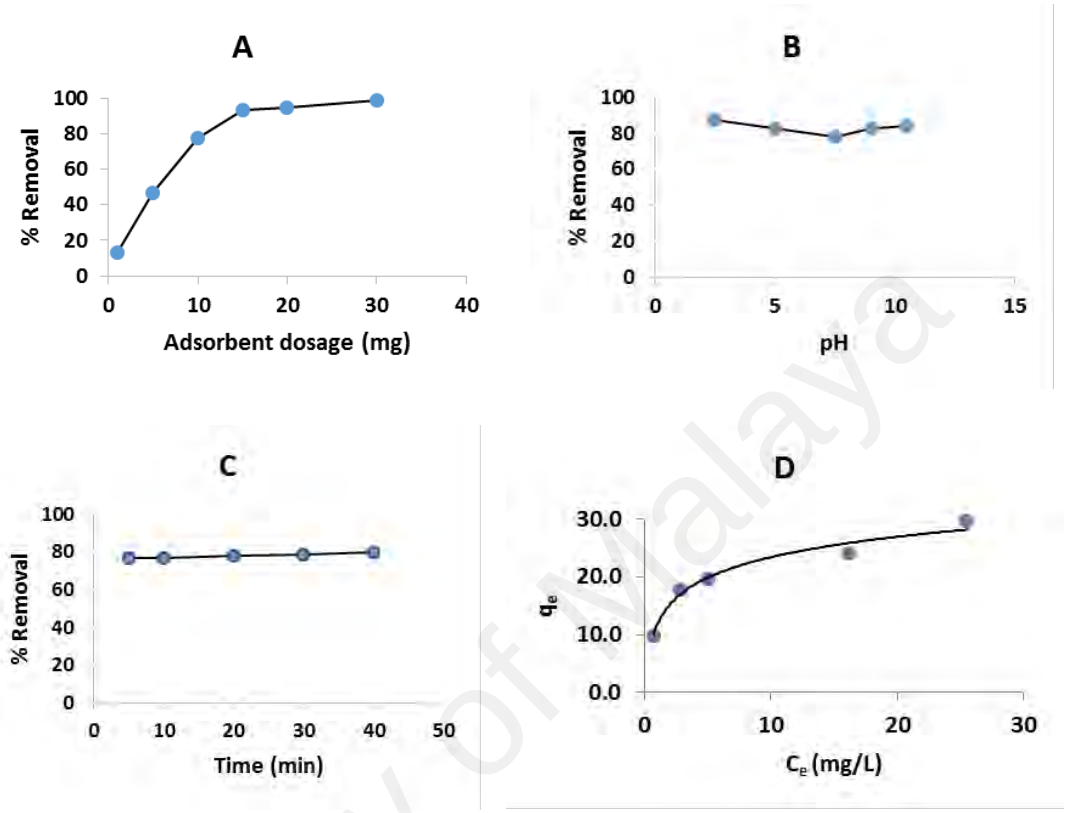

Figure 3.48: (A) Effect of dosages, (B) solution pH (C) adsorption time on the % removal of dye, (D) adsorption capacity.

3.4.2 Adsorption isotherm for CSB on 7

The Langmuir and Freundlich isotherm models were used to investigate the relationship between the adsorption of CSB dye onto **7** and its equilibrium concentration. The Langmuir and Freundlich models demonstrate the monolayer and multilayer adsorption respectively (Equation 3 and 4).

$$\frac{C_e}{q_e} = \frac{C_e}{q_m} + \frac{1}{q_m} \qquad (3)$$

Where: q_e (mg g^{-1}) is the amount of CSB adsorbed at equilibrium, c_e (mg L^{-1}) is the equilibrium CSB concentration q_m (L mg^{-1}) is the Langmuir constant related to the maximum adsorption capacity.

$$ln\, q_e = lnK_F + \left(\frac{1}{n}\right) ln\, C_e \qquad (4)$$

Where: n is the dimensionless exponent of the Freundlich equation and K_F ([(mg/L)/(mg/g)$^{1/n}$]) is the Freundlich constant related to the adsorption capacity. The comparison of R^2 values showed that the adsorption of CSB onto **7** follows the Langmuir isotherm better than the Freundlich model (**Figure 3.49(A),(B)**). The adsorbents **7** showed q_m values (30.769 mg/g, K_L= 0.4119). The K_F values for **7** was observed (11.7482 mg/g, n = 3.50). The applicability of the Langmuir adsorption models suggests the monolayer coverage of SCB on the surface of **7**.

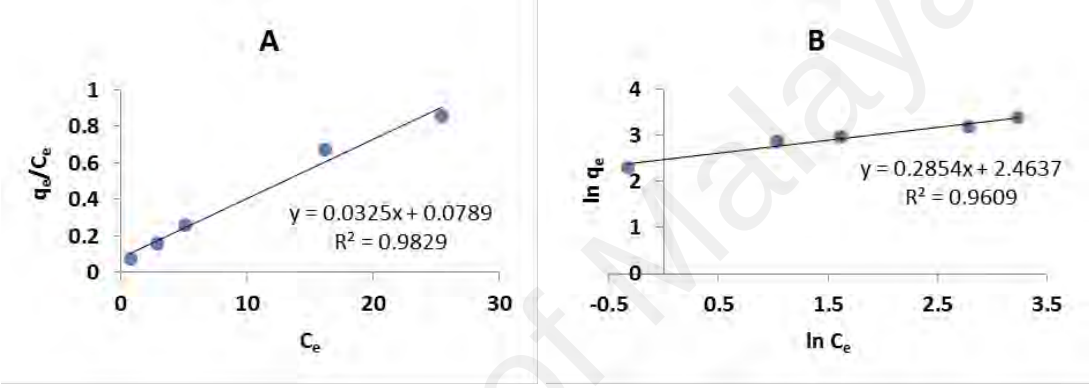

Figure 3.49: (A) Langmuir isotherm (B) Freundlich plots for the adsorption of CSB onto 7.

CHAPTER 4: CONCLUSION

This research was to study on the self-assembly and molecular recognition process of a metal ion, amine ligand and carboxylate linker. The reaction proceeded with an addition of amine ligands to the metal ion solution, thus we expect there will be a protonation of the dicarboxylic acid and the amine, resulted in either cation-metal complexes with carboxylate counter ion or an anion-metal complexes with the protonated amine counter ion. However, due to fast interference of the carboxylate entities, the reaction allow the complexation of amine ligand and carboxylate linkers to metal ion resulted in mixed ligand complexes instead of carboxylate becoming the counter ion. The reaction gave to a series of CPs crystals except **7** which is a dimeric compound; $[Cu(en)(L1)]\cdot L1H_2$ (**1**), $[Cu(en)(L2)(H2O)_2]$ (**2**), $[Ni(en)(L1)(H_2O)_2]\cdot H_2O$ (**3**) , $[Ni(o\text{-}phen)_2(L2)]$ (**4**), $Ni_2(en)_2(L2)_2(H_2O)]$ (**5**), $[Cd(en)(L2)(H_2O)]$ (**6**), and $[Cd_2(o\text{-}phen)_2(L1)(Cl)_2(H_2O)_2]$ (**7**).

Since the yield of some crystal was low due to the self-assembly in the slow evaporation method, the remaining solution was reduced and the precipitates obtained were examined by PXRD. The observed PXRD pattern for the bulk materials of the crystals was found to be consistent with the calculated pattern generated using the single crystal X-ray diffraction and therefore, further characterizations were done using the precipitate.

General characterization showed reasonable melting point values (135.0-275.0°C). The CHN elemental analysis showed values that closely match with the calculated values for each crystal. The spectroscopic studies also confirmed the coordination bonding of the carboxylate linker to the metal ion centre, where the Δ_v values indicated the coordination of the bridging linker to the metal centre; mono- or bidentatate mode of coordination, which in agreement with the IR spectra. These Δ_v were in accordance with the crystal structure; **1** bidentate, **2** monodentate, **3** monodentate, **5** monodentate, **6**

bidentate, and **7** bidentate. The Δ_v of **4** theoretically indicates that the linker is bidentate but in the crystal structure it showed that the L2 linker of **4** coordinated monodentately to the metal centre probably due to other counter ion that existed in the preparation technique. As the sample examined was prepared by precipitating out from the mother liquor solution, crystal **4** also showed a high melting point (340.0-344.0°C). This may be due to the presence of impurities in the bulk powder.

Structural studies showed that the Cu(II) compound resulted in 1-dimensional zigzag polymeric chain (**1** and **2**), whereas Ni(II) compound showed 1-dimensional linear polymeric chain (**3** and **4**) and 3-dimensional polymeric chain (**5**). In addition, Cd(II) compound gave out 2-dimensional polymeric chain (**6**) and 1-dimension dimeric chain (**7).** In terms of geometry, all crystals showed that the metal ions adopted an octahedral geometry, except for Cd(II) (**6)** form pentagonal bypiramidal geometry.

In the crystal structures of **1-6**, the packing were dominated by N–H···O and O–H···O hydrogen bond synthons (distance D···A in the range of 2.57-3.27 **Å)** and in **7,** N–H···Cl with chlorine as acceptor (distance D···A; A=Cl in the range of 3.32-3.43 **Å**) dominated he interaction in the packing. The halogen as the acceptor made a weak hydrogen bonding to the nitrogen from amine ligand. The π-π stacking was observed only in **6** between the ring of L2 linker with the centroid-centroid distance which is in agreement with the literature reported by Janiak (Janiak, 2000).

The prepared CPs were tested with dye activity but only proceeded with the Cd(II) complexes in which crystal **7** showed a high percentage of removal of the CSB dye. Further analysis was done as the solid phase adsorption (SPA) method was optimized through different factors *i.e.*, adsorbent dosage (10mg), solution pH (7.5), adsorption time (15 min) and CSB concentration using 10mg of crystal **7**. In conclusion, crystal **7** showed potential as an adsorbent for the removal of the CSB dye.

REFERENCES

Ai, L., Zhang, C., Li, L., & Jiang, J. (2014). Iron terephthalate metal–organic framework: Revealing the effective activation of hydrogen peroxide for the degradation of organic dye under visible light irradiation. *Applied Catalysis B: Environmental*, *148*, 191–200.

Bai, H. Y., Ma, J. F., Liu, Y. Y., & Yang, J. (2011). Hydrothermal syntheses, crystal structures and topological analyses of four new 3D coordination polymers with mixed ligands. *Inorganica Chimica Acta*, *376*(1), 332-339.

Batten, S. R., Champness, N. R., Chen, X.-M., Garcia-Martinez, J., Kitagawa, S., Öhrström, L., O'Keeffe, M., Suh, M. P., & Reedijk, J. (2013). Terminology of metal–organic frameworks and coordination polymers (IUPAC Recommendations 2013). *Pure and Applied Chemistry*, *85*(8), 1715–1724.

Batten, S. R., Champness, N. R., Chen, X.-M., Garcia-Martinez, J., Kitagawa, S., Öhrström, L., O'Keeffe, M., Suh, M. P., & Reedijk, J. (2012). Coordination polymers, metal–organic frameworks and the need for terminology guidelines. *CrystEngComm*, *14*(9), 3001-3004.

Bis, J. A., & Zaworotko, M. J. (2005). The 2-Aminopyridinium-carboxylate Supramolecular Heterosynthon: a robust motif for generation of multiple-component crystals. *Crystal growth & design*, *5*(3), 1169-1179.

Bisht, K. K., Rachuri, Y., Parmar, B., & Suresh, E. (2014). Mixed ligand coordination polymers with flexible bis-imidazole linker and angular sulfonyldibenzoate: Crystal structure, photoluminescence and photocatalytic activity. *Journal of Solid State Chemistry*, *213*, 43-51.

Braga, D. (2003). Crystal engineering, Where from? Where to?. *Chemical Communications*, (22), 2751-2754.

Brammer, L. (2004). Developments in inorganic crystal engineering.*Chemical Society Reviews*, *33*(8), 476-489.

Bruker. (2005). APEX2. *Bruker AXS Inc., Madison, Wisconsin, USA.*

Choi, K. Y. (2010). Self-assembly of one-dimensional coordination polymer from nickel (II) macrocyclic complex and malonate ligand. *Journal of Chemical Crystallography*, *40*(6), 477-481.

Corey, E. J. (1967). General methods for the construction of complex molecules. *Pure and Applied chemistry*, *14*(1), 19-38.

Desiraju, G. R., & Parshall, G. W. (1989). Crystal engineering: the design of organic solids. *Materials science monographs*, *54*.

Desiraju, G. R. (2007). Crystal engineering: a holistic view. *Angewandte Chemie International Edition*, *46*(44), 8342-8356.

Dolomanov, O. V., Bourhis, L. J., Gildea, R. J., Howard, J. A., & Puschmann, H. (2009). OLEX2: a complete structure solution, refinement and analysis program. *Journal of Applied Crystallography*, *42*(2), 339-341.

Du, J. J., Yuan, Y. P., Sun, J. X., Peng, F. M., Jiang, X., Qiu, L. G., Xie, A.J., Shen, Y.H. & Zhu, J. F. (2011). New photocatalysts based on MIL-53 metal–organic frameworks for the decolorization of methylene blue dye. *Journal of hazardous materials*, *190*(1), 945-951.

Dunitz, J. D. (1991). Phase transitions in molecular crystals from a chemical viewpoint. *Pure and applied chemistry*, *63*(2), 177-185.

Etter, M. C., MacDonald, J. C., & Bernstein, J. (1990). Graph-set analysis of hydrogen-bond patterns in organic crystals. *Acta Crystallographica Section B: Structural Science*, *46*(2), 256-262.

Fournier, J. H., Maris, T., Wuest, J. D., Guo, W., & Galoppini, E. (2003). Molecular tectonics. Use of the hydrogen bonding of boronic acids to direct supramolecular construction. *Journal of the American Chemical Society*,*125*(4), 1002-1006.

Gupta, V. K. (2009). Application of low-cost adsorbents for dye removal–A review. *Journal of environmental management*, *90*(8), 2313-2342.

Hu, B., Zhao, J., Yang, Q., Zhang, X., & Bu, X. (2009). Synthesis, structure and magnetic properties of two new coordination polymers with carboxylate-substituted benzoimidazole ligands. *Science in China Series B: Chemistry*,*52*(9), 1451-1455.

Janiak, C. (2000). A critical account on π–π stacking in metal complexes with aromatic nitrogen-containing ligands. *Journal of the Chemical Society, Dalton Transactions*, (21), 3885-3896.

Jin, S., Wang, D., & Xu, Y. (2012). Five new metal (II) complexes with 3-D network structures based on carboxylate and bis (imidazole) ligands: syntheses and structures. *Journal of Coordination Chemistry*, *65*(11), 1953-1969.

Kukovec, B. M., Venter, G. A., & Oliver, C. L. (2011). Structural and DFT studies on the polymorphism of a cadmium (II) dipicolinate coordination polymer. *Crystal growth & design*, *12*(1), 456-465.

Lehn, J. M. (1988). Supramolecular chemistry—scope and perspectives molecules, supermolecules, and molecular devices (Nobel Lecture).*Angewandte Chemie International Edition in English*, *27*(1), 89-112.

Li, L., Liao, D., Jiang, Z., & Yan, S. (2001). Synthesis, structure and magnetic properties of a one-dimensional chain complex {[Cu (dmbpy)(N 3)] 2 (ta)} 2CH 3 OH· 2H 2 O. *Journal of Molecular Structure*, *597*(1), 157-162.

Liu, B., Zhao, D., Li, T., & Meng, X. R. (2013). Syntheses, structures, and fluorescent properties of two new Zn (II) coordination polymers containing 2-((benzoimidazol-yl) methyl)-1 H-tetrazole. *Journal of Coordination Chemistry*,*66*(1), 139-151.

Liu, X., Liu, K., Yang, Y., & Li, B. (2008). Syntheses, structures and luminescence of zinc and cadmium coordination polymers with bis (1, 2, 4-triazol-1-yl) butane and benzenedicarboxylate. *Inorganic Chemistry Communications*, *11*(10), 1273-1275.

Macrae, C. F., Bruno, I. J., Chisholm, J. A., Edgington, P. R., McCabe, P., Pidcock, E., Rodriguez-Monge, L., Taylor, R., van de Streek, J., & Wood, P. A. (2008). Mercury CSD 2.0–new features for the visualization and investigation of crystal structures. *Journal of Applied Crystallography*, *41*(2), 466-470.

Mesubi, M. A. (1982). An infrared study of zinc, cadmium, and lead salts of some fatty acids. *Journal of Molecular structure*, *81*(1-2), 61-71.

Nangia, A. (2010). Supramolecular chemistry and crystal engineering.*Journal of chemical sciences*, *122*(3), 295-310.

Okubo, T., Anma, H., Tanaka, N., Himoto, K., Seki, S., Saeki, A., Maekawa, M., & Kuroda-Sowa, T. (2013). Crystal structure and carrier transport properties of a new semiconducting 2D coordination polymer with a 3, 5-dimethylpiperidine dithiocarbamate ligand. *Chemical Communications*, *49*(39), 4316-4318.

Oxford Diffraction. (2013). CrysAlis Pro. *Oxford Diffraction Ltd., Abingdon, Oxfordshire, England.*

Palatinus, L., & Chapuis, G. (2007). Superflip–a computer program for the solution of crystal structures by charge flipping in arbitrary dimensions.*Journal of Applied Crystallography*, *40*(4), 786-790.

PANalytical, B. V. (2009). *X'Pert HighScore Plus* (Vol. 3). Version.

Planeix, J. M., Jaunky, W., Duhoo, T., Czernuszka, J. T., Hosseini, M. W., & Brès, E. F. (2003). A molecular tectonics–crystal engineering approach for building organic–inorganic composites. Potential application to the growth control of hydroxyapatite crystals. *Journal of Materials Chemistry*, *13*(10), 2521-2524.

Robin, A. Y., & Fromm, K. M. (2006). Coordination polymer networks with O-and N-donors: What they are, why and how they are made. *Coordination Chemistry Reviews*, *250*(15), 2127-2157.

Schmidt, G. M. J. (1971). Photodimerization in the solid state. *Pure and Applied Chemistry*, *27*(4), 647-678.

Sheldrick, G. M. (2008). A short history of SHELX. *Acta Crystallographica Section A: Foundations of Crystallography*, *64*(1), 112-122.

Shibata, Y. (1916). CAN 11:5339. *Journal of the College of Science, Imperial University of Tokyo*, *37*, 1–17.

Spek, A. L. (2009). Structure validation in chemical crystallography. *Acta Crystallographica Section D: Biological Crystallography*, *65*(2), 148-155.

Sun, D., Cao, R., Liang, Y., Shi, Q., Su, W., & Hong, M. (2001). Hydrothermal syntheses, structures and properties of terephthalate-bridged polymeric complexes with zig-zag chain and channel structures. *Journal of the Chemical Society, Dalton Transactions*, (16), 2335-2340.

Van de Voorde, B., Bueken, B., Denayer, J., & De Vos, D. (2014). Adsorptive separation on metal–organic frameworks in the liquid phase.*Chemical Society Reviews*, *43*(16), 5766-5788.

Wang, G. H., Li, Z. G., Jia, H. Q., Hu, N. H., & Xu, J. W. (2008). Topological diversity of coordination polymers containing the rigid terephthalate and a flexible N, N′-type ligand: interpenetration, polyrotaxane, and polythreading.*Crystal Growth and Design*, *8*(6), 1932-1939.

Wang, X. L., Chen, Y., Liu, G., Lin, H., & Zhang, J. (2009). Two novel copper (II) complexes constructed from dicarboxylate ligands with different spacer lengths and 2-phenylimidazo [4, 5-f] 1, 10-phenanthroline (PIP): Synthesis, structures and properties. *Solid State Sciences*, *11*(9), 1567-1571.

Wang, X. P., Han, L. L., Lin, S. J., Li, X. Y., Mei, K., & Sun, D. (2016). Synthesis, structure and photoluminescence of three 2D Cd (II) coordination polymers based on varied dicarboxylate ligand. *Journal of Coordination Chemistry*, *69*(2), 286-294.

Wen, G. L., Wang, Y. Y., Zhang, W. H., Ren, C., Liu, R. T., & Shi, Q. Z. (2010). Self-assembled coordination polymers of V-shaped bis (pyridyl) thiadiazole dependent upon the spacer length and flexibility of aliphatic dicarboxylate ligands. *CrystEngComm*, *12*(4), 1238-1251.

Li, H., Eddaoudi, M., O'Keeffe, M., & Yaghi, O. M. (1999). Design and synthesis of an exceptionally stable and highly porous metal-organic framework. *Nature*, *402*(6759), 276-279.

Yagub, M. T., Sen, T. K., Afroze, S., & Ang, H. M. (2014). Dye and its removal from aqueous solution by adsorption: a review. *Advances in colloid and interface science*, *209*, 172-184.

Yan, L., Li, C. B., Zhu, D. S., & Xu, L. (2012). Syntheses, Structures, and Luminescent Properties of Two Novel Coordination Polymers with Poly-Carboxylate and N-Heterocyclic Ligands. *Journal of Inorganic and Organometallic Polymers and Materials*, *22*(1), 235-243.

Yang, L., Peng, Y., Bian, F., Yan, S. P., Liao, D. Z., Cheng, P., & Jiang, Z. H. (2005). Structure and magnetic properties of a dinuclear complex [Cu2 (TPA) 2 (o-phth)](ClO4) 2. *Journal of Chemical Crystallography*, *35*(7), 555-559.

Ye, B. H., Tong, M. L., & Chen, X. M. (2005). Metal-organic molecular architectures with 2, 2′-bipyridyl-like and carboxylate ligands. *Coordination chemistry reviews*, *249*(5), 545-565.

Zhang, J. W., Kan, X. M., Li, X. L., Luan, J., & Wang, X. L. (2015). Transition metal carboxylate coordination polymers with amide-bridged polypyridine co-ligands: assemblies and properties. *CrystEngComm*, *17*(21), 3887-3907.

Zhao, X., Liu, S., Tang, Z., Niu, H., Cai, Y., Meng, W., Wu, F., & Giesy, J. P. (2015). Synthesis of magnetic metal-organic framework (MOF) for efficient removal of organic dyes from water. *Scientific reports*, *5*.

LIST OF PUBLICATIONS AND PAPERS PRESENTED

List of Publication

1. Wannur S. K. Ab Rahman, J. Ahmad and Siti Nadiah Abdul Halim. Structural Studies of Self-Assembled Ni(II) and Cu(II) Coordination Polymers Fabricated With Amine Ligands And Dicarboxylic Acid Linkers. *Journal of Chemical Crystallography*. (Submitted).

List of conference/ symposium/ seminar attended:

1. 4th Asian Conference of Coordination Chemistry, Jeju International Convention Center, Jeju South Korea, 2013. (Poster presenter).

2. University of Malaya Chemical Crystallography Symposium 2014. (Poster presenter).

3. Exchange student at Chulalongkorn University, Thailand awarded by ASEAN Scholarships Program of Chulalongkorn University, Thailand, 2014. (Participant).